2014

Hurricane-Induced Geologic Change and Palynological Assessment of a Rapidly Subsiding Deltaic Environment in Coastal Louisiana

James Dustin Naquin
Louisiana State University and Agricultural and Mechanical College

HURRICANE-INDUCED GEOLOGIC CHANGE AND PALYNOLOGICAL ASSESSMENT OF A RAPIDLY SUBSIDING DELTAIC ENVIRONMENT IN COASTAL LOUISIANA

A Thesis

Submitted to the Graduate Faculty of the
Louisiana State University and
Agricultural and Mechanical College
in partial fulfillment of the
requirements for the degree of
Master of Science

in

The Department of Oceanography and Coastal Sciences

by
James Dustin Naquin
B.S., Louisiana State University, 2012
December 2014

To my brother Derek, who taught me
how to reach for the seemingly unattainable

ACKNOWLEDGEMENTS

There are many, many people to whom I am greatly indebted to for their contribution and influence during the process of completing this thesis, however, I would first like to thank my advisor Dr. Kam-biu Liu for his guidance and enthusiasm during the later years of my undergraduate degree and throughout my research as a graduate student. Without his support I would not have been able to further my education at Louisiana State University. I would like to acknowledge that this research was funded by a grant supplied by the National Science Foundation (Grant Number: CNH 1212112) and the Louisiana Sea Grant program. I would also like to sincerely thank the other members of my thesis committee, Dr. Kanchan Maiti and Dr. Kehui Xu for their patience and assistance during this research.

Secondly, I would like to thank my fellow colleagues in the Global Change and Coastal Paleoecology lab in the Department of Oceanography and Coastal Sciences. Dr. Terrence McCloskey, Dr. Thomas Bianchette, and Qiang Yao have been a tremendous help throughout the process of completing this thesis. I would also like to thank Laura Basirico for her aid in the MC252 contamination analysis and Puspa Adhikari for his help in isotope analysis. In addition, I would like to give special thanks to Drs. Jaye Cable and Vince Wilson for their hard work and devotion in developing such a high caliber undergraduate program in the Department of Oceanography and Coastal Sciences. This intensive program has played an integral role in propelling me into success as a graduate student and young researcher.

Finally, I would like to show the greatest amount of gratitude to my family. Their love and support over the years has encouraged me to overcome any adversity I encounter in life.

TABLE OF CONTENTS

LIST OF TABLES

LIST OF FIGURES

ABSTRACT

This study is focused on a paleoenvironmental history of a backbarrier coastal lagoon situated on the seaward margin of the Lafourche delta lobe in coastal Louisiana. A 2.2 meter long sediment core (Core BC 53) was collected from a mangrove-covered land strip on the northern margin of Bay Champagne, and was studied using pollen analysis, Loss-on-ignition (LOI), X-ray Fluorescence (XRF) analysis, and Cesium-137 and radiocarbon dating techniques to establish sediment stratigraphy and core chronology.

Bay Champagne, a backbarrier lagoon formed during the evolution of Bayou Lafourche, has shown to be highly sensitive to geomorphological and vegetation changes induced by sea-level rise as noted by palynological, paleotempestological, and sedimentological records. In addition to capturing the rise and fall of the Lafourche delta lobe, Core BC 53 also preserved hurricane-induced sedimentary record.

Pollen data revealed that Bay Champagne is mainly characterized by coastal marsh taxa. Freshwater marsh was dominant during the active period of the Lafourche delta about 1600 years ago. This was followed by a shift to salt marsh during its deterioration phase around 300 years ago. *Avicennia germinans* (black mangrove) emerged within the stratigraphy around 1880 A.D., which shows a direct correlation to relative sea-level rise.

LOI and XRF data uncovered the presence of four hurricanes. Storm layers were not overwashed from the beach barrier due to its far distance from the coring site; however, these sedimentary signatures originated from the center of Bay Champagne and fluvial regions north of the lagoon. The distinct increase in charcoal concentration and decrease in arboreal pollen following Layer B implies the occurrence of wildfires induced by the hurricane. This is comparable to the results in Liu et al. (2008), which recorded three hurricane-induced fire linkages in coastal Alabama. Geological changes caused by Hurricane Isaac (September 2012) are found in the upper 3 cm of the core. This storm produced extensive fluvial flooding to the area as shown by LOI and XRF. These findings from Hurricane Isaac may provide a modern analog for interpreting the impacts of prehistoric hurricanes in sediment stratigraphic studies from this coastal region.

CHAPTER 1. INTRODUCTION

Coastal wetlands are multi-functional systems that not only serve as a vital sink for the global carbon budget, but also provide a highly productive habitat to flora and fauna, as well as create a natural buffer zone for inland areas against destructive forces associated with tropical cyclones (Day et al., 2007; Neill and Deegan, 1986). However, current eustatic sea-level rise combined with anthropogenic modifications of wetland structures have yielded rapid rates of subsidence in many coastal zones such as the Mississippi River deltaic plain of Louisiana (USA) (Blum and Roberts, 2009). This area is unique in comparison to other coastal zones along the northern Gulf of Mexico as it is characterized by inundated or saturated soils that have developed over the past 7000 years while being highly susceptible to hurricane influence. During this time, the lower Mississippi River has diverted its water and sediment into five different directions creating six deltaic lobes. This avulsion cycle repeats itself approximately every 1000-1500 years (Day et al., 2007). Following the termination of a deltaic lobe, the underlying sediment is subjected to compaction, followed by subsidence, and eventual erosion. Although many numerical values of subsidence are highly debated, it is widely known that south Louisiana currently possesses the most rapidly retreating coastline in the entire northern Gulf of Mexico (Day et al., 2000; Penland and Ramsey, 1990; Turner, 1991). Therefore, to accurately predict the fate of Louisiana's wetlands and mitigate future coastal hazards, a comprehensive

understanding of hurricane and vegetation histories, past sea-level fluctuations, and sediment dynamics must be achieved.

The primary objective of this study focuses on reconstructing detailed paleoenvironmental and depositional histories of a backbarrier coastal lagoon of the Lafourche deltaic lobe. The key methodology used to illustrate long-term environmental changes of this area involved geochemical and pollen analyses of a 2.3 m sediment core taken from Bay Champagne, a backbarrier coastal lagoon located approximately 0.5 km southeast of Port Fourchon, Louisiana. Through evaluating these records, the effects that deltaic lobe avulsion, sea-level rise, and subsidence have on vegetation are studied.

Another objective of this study is to reconstruct the hurricane history of Bay Champagne and the lower Lafourche deltaic lobe through evidence found in the sediment stratigraphy while developing possible modern analogs by using isotopic and radiocarbon dating techniques. This area is highly susceptible to damaging forces induced by hurricane strikes (i.e., wind and storm surge). Previous studies have shown that Bay Champagne has served as an active repository for hurricane-induced geologic changes, however, records incorporating pollen analysis of this area were lacking until now (Liu et al., 2010, Naquin et al., 2014).

The final objective of this thesis involves recording the timeline regarding the arrival and establishment of *Avicennia germinans* (black mangrove) in south Louisiana. The black mangrove has been widely used as a key indicator to environmental stresses such as climate change and sea-level rise. This study

establishes the history of *Avicennia germinans* near Bay Champagne through pollen analysis.

This thesis contains seven chapters. Chapter 1 is an introduction that briefly explains the problem at hand. Chapter 2 is a literature review that provides background information on long-term climate change, palynology, paleotempestology, and the environmental setting of south Louisiana. Chapter 3 is an in-depth description of the study site. The main purpose of Chapter 4 is to provide a detailed review of the methodologies employed throughout this research. Chapter 5 presents the results obtained from the geochemical, palynological, and chronological analyses. Chapter 6 is a discussion and synthesis chapter that includes the paleoenvironmental interpretations of the data sets. Chapter 7 presents a summary of the results and overarching conclusions from this thesis.

CHAPTER 2. LITERATURE REVIEW

2.1 Long-term Global Climate Change

Throughout Earth's 4.5 billion years of existence, it has experienced tremendous and continuous environmental changes over a wide spectrum of temporal and spatial scales, including five distinct ice ages lasting millions of years. Each ice age is a period of geologic time in which there is a long-term decrease in global temperature, resulting in continental ice sheet expansion. The earliest ice age is believed to have occurred over 2 billion years ago while the latest ice age began during the late Cenozoic time, especially during the early Pleistocene. Terrestrial evidence for glacial phases is frequently discontinuous and of poor temporal resolution; however, isotopic data (Fairbanks, 1989; Fleming et al., 1998; Lambeck, Yokoyama, and Purcell, 2002) obtained from ice cores and marine sediments (Mahowald et al., 1999) provided high-resolution and detailed records of cooling and warming periods during the Pleistocene.

An important driving mechanism for episodic climate changes is insolation variations caused by changes in the Earth's position and movement in relation to the sun called Milankovitch cycles (Kutzbach, 1985). These processes vary by frequency and the earth's orbital path: the precession of equinoxes or change in the orientation of rotational axis (with a period of ~23,000 years), oscillation of the earth's axial tilt (~41,000 years), and the eccentricity of orbit (~100,000 years).

2.1.1 The Pleistocene

The term *Pleistocene* was first introduced by Sir Charles Lyell in 1839 to describe strata in Italy that had at least 70% of their molluscan fauna living in the present day (Smithsonian National Museum of Natural History, 2014). During the Pleistocene Epoch (~ 2.5 MY – 10,000 years BP), the earth experienced drastic swings in climate causing prolonged glacial periods and warmer interglacial phases. These glacial advances and retreats directly shaped the topography, flora, and fauna in North America and other parts of the globe. Of main concern within this thesis are the most recent four continental glaciations that occurred during the latter part of the Pleistocene. These drastic fluctuations in climate have shown to be directly related to sea level change during the Pleistocene.

The Wisconsinan glaciation was a glacial period that lasted from approximately 90,000 to 11,000 years BP (Before Present, where present is 1950 A.D.). During this time, an ice sheet complex linked present day Greenland to Canada and extended into the United States. Of the four major ice sheets (Cordilleran, Innuitian, Greenland, and Laurentide) in North America, the Laurentide ice sheet was the largest and covered the high latitudes of central and eastern North America. Thousands of cubic kilometers of freshwater were discharged each year into surrounding oceans by the melting Laurentide ice sheet. This process would often suppress oceanic circulation in the Atlantic, triggering abrupt climate change (Murton et al., 2010). Among these climate change events was the Last Glacial Maximum (LGM), a period during the Wisconsinan glacial

period when ice sheet expansion was at its most recent maximum. During this period (~ 21,000 years BP), nearly half of North America, including parts of northern Europe and Asia, became covered with ice in response to decreases in northern summer insolation, tropical Pacific sea surface temperatures, and atmospheric CO_2. This greatly impacted the Earth's climate causing extended drought, expansion of deserts, and a dramatic drop in eustatic sea level (Clark et al., 2009).

The termination of the Wisconsinan glacial period is marked by a warming phase termed the Bolling-Allerod interstadial in which North American ice sheets began to diminish. Climate change distinguishing this event has been interpreted through palynological data from the Netherlands (Hoek, 1997), oxygen isotopes from Greenland ice cores (Figure 1) (Johnsen et al., 1992) and Central Britain Coleoptera data (Atkinson et al., 1987). Following this period, the Younger Dryas (12,800-11,500 years BP) was a brief time in which colder climatic conditions and drought occurred. Named after its indicator plant, *Dryas octopetala*, the Younger Dryas is believed to have been caused by meltwater pulses from the collapse of North American ice sheets. Although past research has shown there is no geologic evidence, one widely used theory is that the Younger Dryas was caused by sudden flux of freshwater from Lake Agassiz to the North Atlantic (Broecker, 2006). This is believed to have shut down the North Atlantic Deep Water formation in global conveyor belt and the thermohaline circulation causing a cooling response in climate.

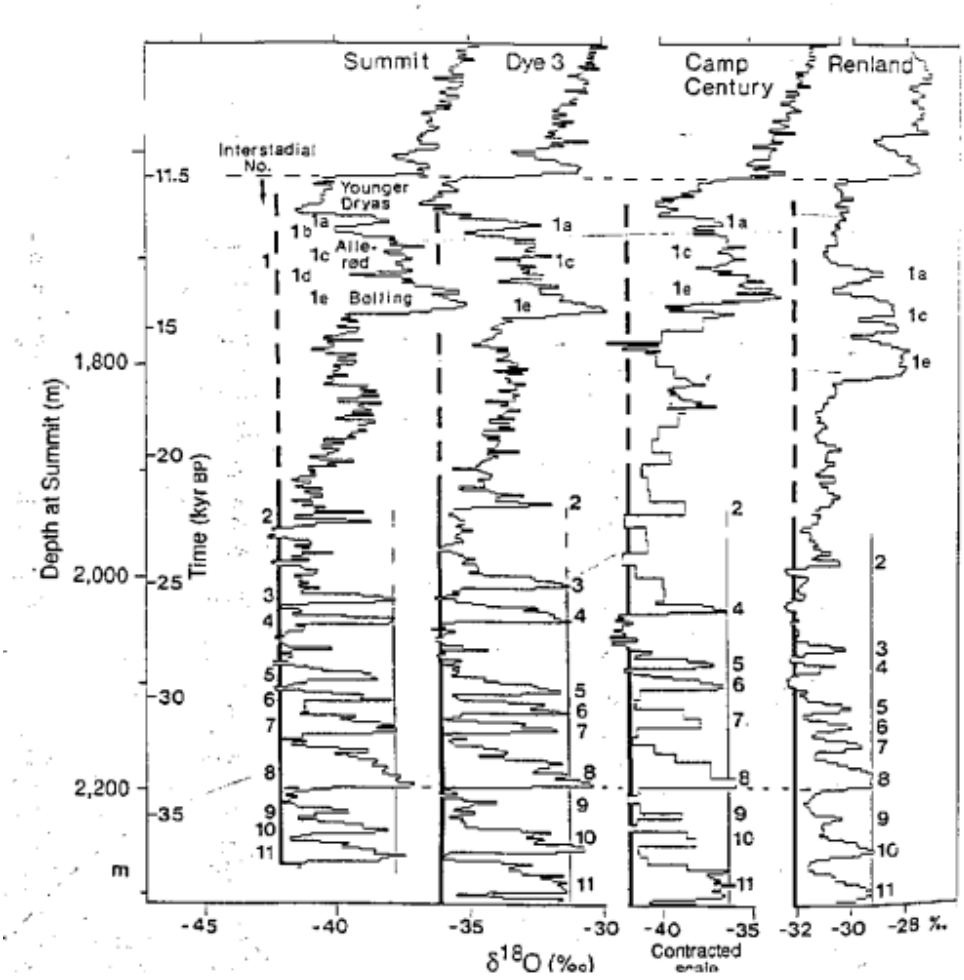

Figure 1: Oxygen isotope data from GRIP ice cores. After Johnsen et al. (1992)

2.1.2 The Holocene

The Holocene (11,700 years BP - present) is the current geological epoch and has been identified as an interglacial during the present ice age. Mayewski et al. (2004) identified six periods of significant climate change during the Holocene, each occurring at intervals of approximately 2800-2000 and 1500 years. This timing of climate change events has been well established in other literature as well (Bond et al., 1997, 2001; Stuiver and Braziunas, 1989). Among this sequence of events, the Hypsithermal was a period of warmer climate during the Holocene and is thought to have lasted from 7,000-4,000 years BP in central and eastern North America (Deevey and Flint, 1957). While this was not a global phenomenon, average temperature change appeared to diminish with decreasing latitude so that there was essentially no change in temperature at middle and low latitudes (Davis et al., 2003).

Although it is still of much debate on whether the Medieval Warm Period (800-1200 AD) was a regional or global occurrence, there is clear evidence through multiple proxies and recorded human exploration that this warming episode affected multiple areas in Northern and Southern Hemispheres. The most extensive glacial records of this period derive from the Swiss Alps in which multiple tree trunks were found within 300 m of glacial ice indicating that there was a distinct warming period preceding the present advance of ice (Rothlisburger, 1980). A similar instance was found by Villalba (1994) in the South Patagonian icefield. Historical records show that grapes suitable for making wine were being grown in

England and in Scandinavia the tree line was reportedly 100-200 m higher than present (Crowley and Lowery, 2000). Not only did warmer climate during the Medieval Warm Period have a direct effect on the flora, but also allowed the expansion of human populations in Northern Europe.

Following the Medieval Warm Period, an abrupt cooling phase reshaped the extent of glacial regions in Europe and had significant practical consequences for its human populations. This shift in climate was coined the term *Little Ice Age* by F Matthes in 1939 to describe the intense series of glacial advances during the Late Holocene. Since then, such evidence of glacial activity during this period has been well recorded in the literature (Beget, 1983; Grove and Switsur, 1994; Villalba, 1994). Richie et al. (2007) developed a 1,400-year multiproxy record of climate change from the northern Gulf of Mexico by pairing Mg/Ca and $\delta^{18}O$ analyses of foraminifer assemblages. This indicated that sea surface temperatures of the Gulf of Mexico were 2-2.5 °C below modern values. Historical documents show damages to numerous farms and villages in the Chamonix valley near Mont Blanc, France caused by an advancing nearby glacier. Regional variability in climate during the Little Ice Age has been linked to changes in atmospheric circulation patterns, more specifically the North Atlantic Oscillation (Mann, 2002). The North Atlantic Oscillation is a climatic phenomenon of atmospheric pressure fluctuations between the Icelandic low and the Azores high. This instability of pressure controls the strength and direction of westerly winds across the North Atlantic and has been suggested as having strong influence on European winter temperatures. Similar to

the climate-induced societal changes caused by the Medieval Warm Period and Little Ice Age, south Louisiana coastal inhabitants have been forced to adapt to their climate-driven environmental setting in recent times.

2.2 Environmental Setting

During the Pleistocene, the Mississippi River served as the primary conduit for transporting meltwater and sediment discharged from ice sheets covering present-day Canada and the northern United States. The termination of the Last Glacial Maximum is thought to have been the precursor to the most recent phase of eustatic sea level rise (Figure 2). This played a significant role in glacio-eustatic sea level fluctuations. Most agree on at least four and five major low and high sea level stands during Pleistocene (Gosselink, 1984). These shifts in sea level have been correlated with cutting and filling alluvial pathways in the Mississippi River (Fisk, 1956). While providing a geomorphic mechanism for transforming the shape of the river, sea level change also aided in relocating the site of sediment deposition on spatial and temporal scales. During times of falling sea level, the river deltaic deposition shifts seaward. Conversely, rising sea level moves sediment deposition landward (Gosselink, 1984). These landward-seaward shifts of river depocenters resulted in repeated downbowing and subaqueous subsidence along the continental shelf of Louisiana, thereby inhibiting the formation of a deltaic complex during the Pleistocene (Coleman, 1988).

Of the multiple glacial advances and retreats in North America, the most well-documented and largest glacial runoff phase is represented by the meltwater

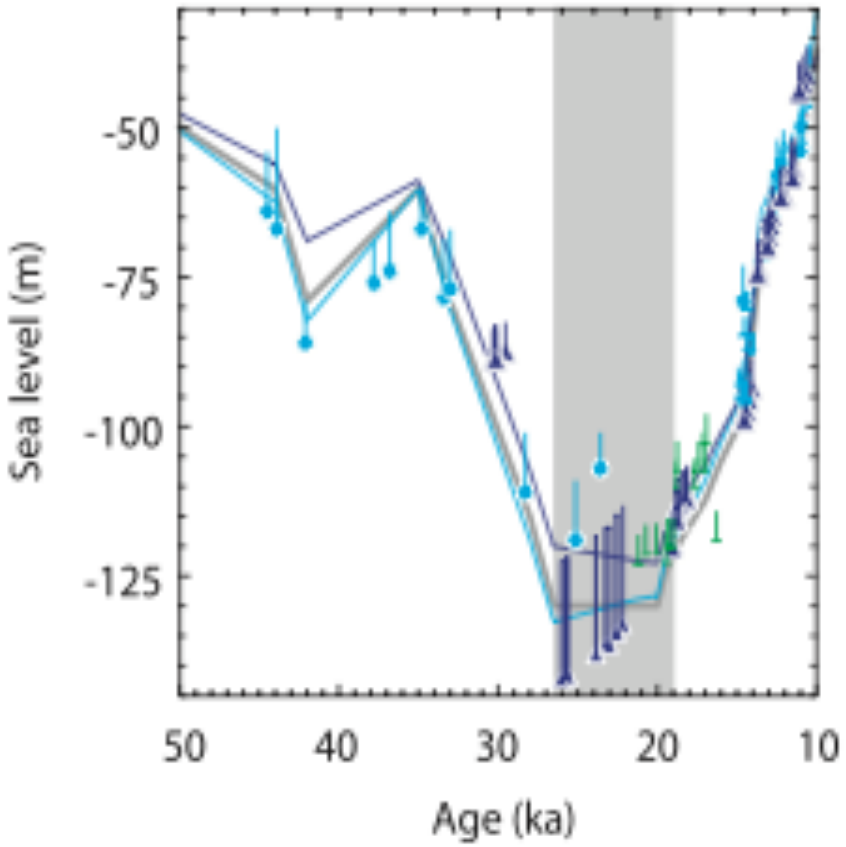

Figure 2: Relative sea-level data combined with predictions with New Guinea (blue line) and Barbados (purple line). Eustatic sea-level time series is denoted by grey line. The vertical gray bar indicates the period of the Last Glacial Maximum. After Clark et al., (2009).

pulse from the Laurentide ice sheet to the Gulf of Mexico. Between 17,000 and 13,000 years BP approximately 18 x 10^6 km^3 of meltwater was injected into the Gulf of Mexico from Canada via the Mississippi River (Brown and Kennett, 1998). Such extreme meltwater discharge events have been linked to establishing an extensive complex of mid-continental spillways while causing geomorphic shifts between meandering and braided belts within the Mississippi River (Kehew and Lord, 1987). Sedimentary evidence showed that the lower Mississippi River abruptly switched from a braided stream to its current meandering state during the last interglacial period (Rittenour, Blum, and Goble, 2007). The Mississippi River entrenched its valley and developed multiple channels along the continental shelf, thus resulting in the deposition of alluvial material near the shelf break (Coleman, 1988). As sea level began to stabilize, the Mississippi River shifted its discharge to the alluvial valley, marking the construction of its modern deltaic complex.

Accumulated sediments deposited near the lower Mississippi River form deltaic systems that undergo a regressive (constructive) followed by a transgressive (destructive) phase (Penland, Boyd, and Suter, 1988). The Mississippi Deltaic complex has been defined in recent literature as a dynamic system structured by intercalated “lobes” that consist of low upland ridges, wetlands, and water (Blum et al., 2000; Blum and Roberts, 2009; Day et al., 2007). The formation of the first Mississippi River delta emerged approximately 6000-7000 years BP following the termination of the LGM. Throughout its existence, it has avulsed a new deltaic lobe every 1000-1500 years (Day et al., 2007). Chronostratigraphic data have shown five

major shifts in alluvial pathways resulting in a total of six different Holocene delta formations (Figure 1) that cover an area of ~30,000 km^2 and comprises 41% of the coastal wetlands in the United States (Coleman, Roberts, and Stone, 1998). The six deltaic lobes are named: (1) Maringouin, (2) Teche, (3) St. Bernard, (4) Lafourche, (5) Balize, and (6) Atchafalaya (Figure 1). According to Blum and Roberts (2009) and Day et al. (2007), these lobes undergo a geological cycle of development, consisting of initiation of a new delta, growth, termination, and eventual deterioration. A timeline and graphic representation of this process is provided by Roberts (1997) in Figure 2.

Deltaic "avulsion", or the redirection of alluvial material and freshwater, is known to play an integral role in the development of continental interior floodplains, as well as deltaic plains situated along coastal settings. This process also determines the course of a river, controls the rates of sediment accumulation on the local scale, and stimulates change among floodplain topography and alluvial design (Aslan, Autin, and Blum, 2000). Although the exact mechanisms that drive avulsion are still unclear, it typically consists of two phases: (1) a decrease in stability of the river structure toward the avulsion threshold and (2) a triggering event (i.e., flood) (Jones and Schumm, 1999).

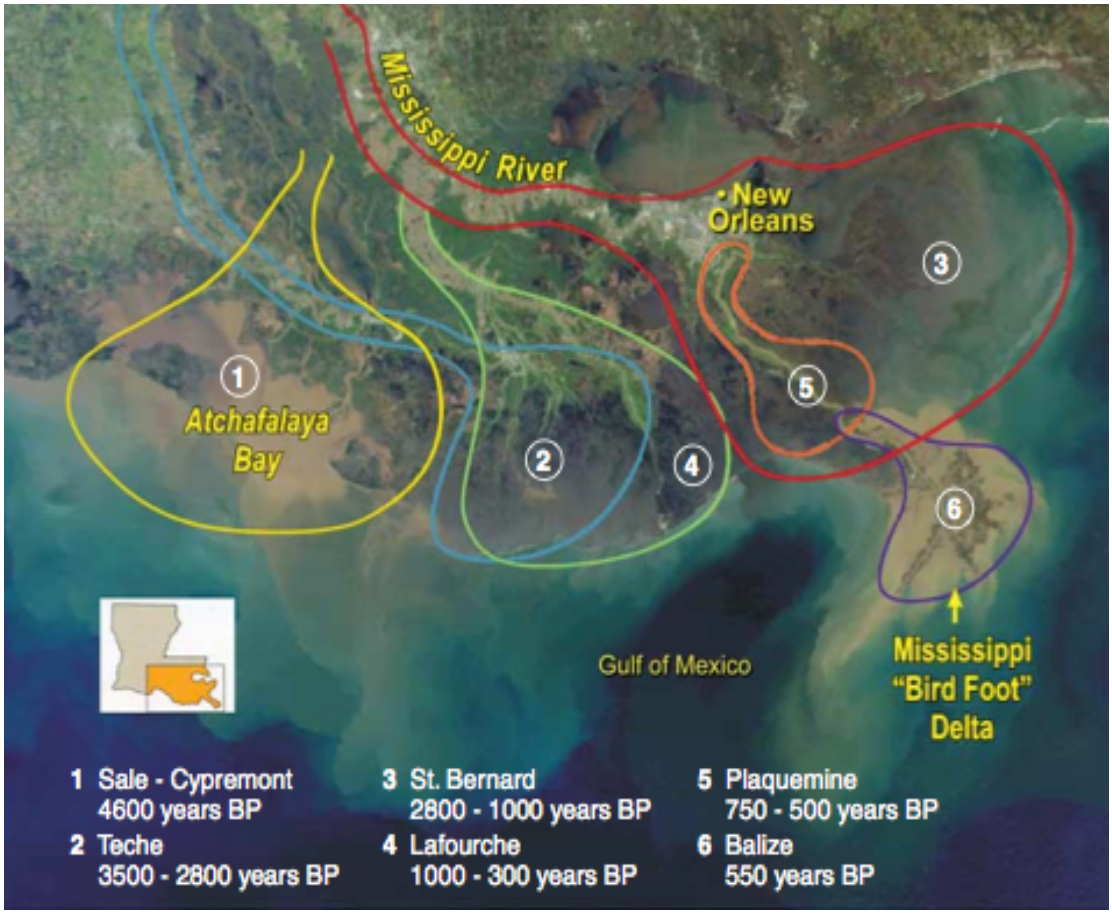

Figure 3: Aerial view of the Mississippi delta plain showing the six overlapping deltaic lobes and their respective active periods (After Day et al., 2007).

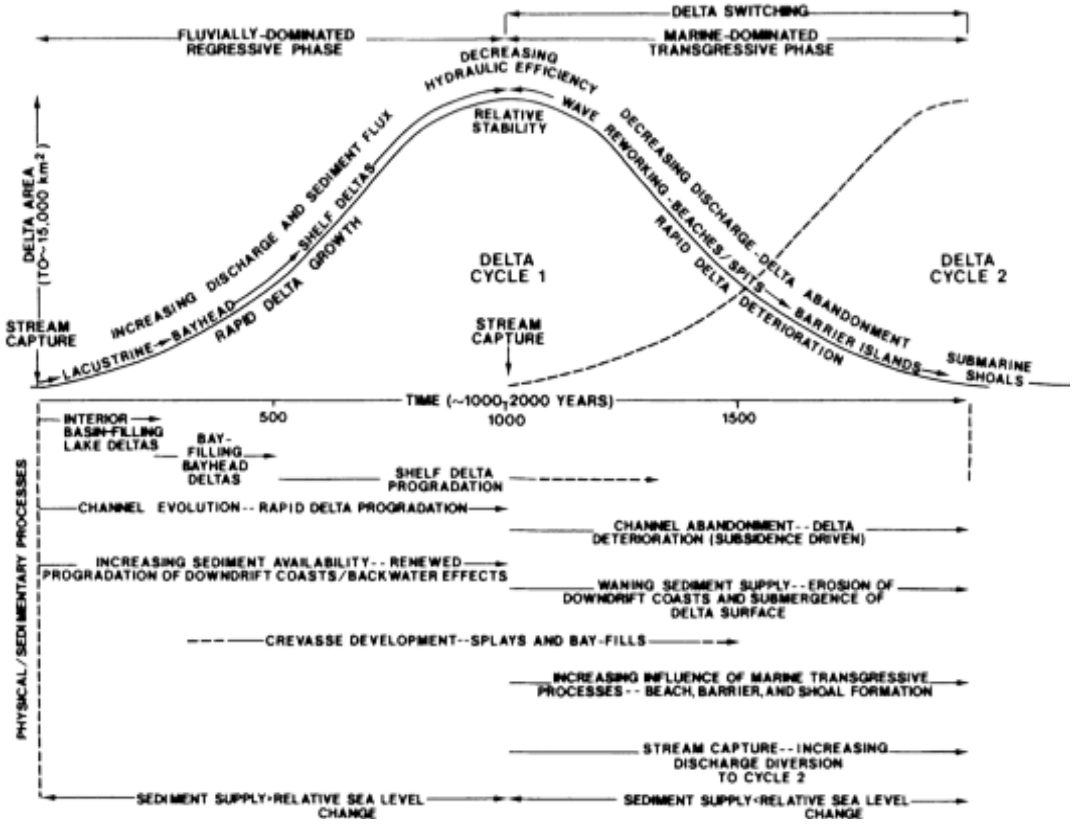

Figure 4: Spatial and temporal changes in the lifecycle of a delta lobe (After Roberts, 1997).

The first phase involving the creation of a new delta requires the availability of large amounts of sediment and begins with the filling of inland lakes through subaqueous deposition and subaerial development (Roberts, 1997). Once lacustrine regions have used their accommodation space, water and sediment is then pushed further towards the coast and continental shelf. This initiates a second segment of sustained land accretion. Scruton (1960) thoroughly explained the processes involving the progradation of a delta. Distributaries prograde seaward and deposit sediments at a rate that must overcome relative rising sea level. This is vital in coastal Louisiana, where subsidence contributes to a relative sea-level rise of ~ 1 cm/year (Day et al., 2007). Once a delta has successfully been established, a series of hydrodynamic processes take place to sustain and increase its overall area and volume. Overbank flooding gives rise to the formation of short-lived (<100 years) crevasse splays of about 10-15 km in length and are typically composed of mostly fine grained sediments (active delta, Figure 3; Penland, Boyd, and Suter, 1988). This seaward deposition is continued along the margin of the delta lobe until the river's hydraulic gradient becomes too weak to effectively displace material to the Gulf of Mexico (Coleman, 1988). When seasonal and annual flooding events are no longer present, overbank flooding diminishes, and the subaerial delta becomes susceptible to marine inundation. This abandonment leads to the initiation of the deltaic transgressive stage (stage 1, Figure 3).

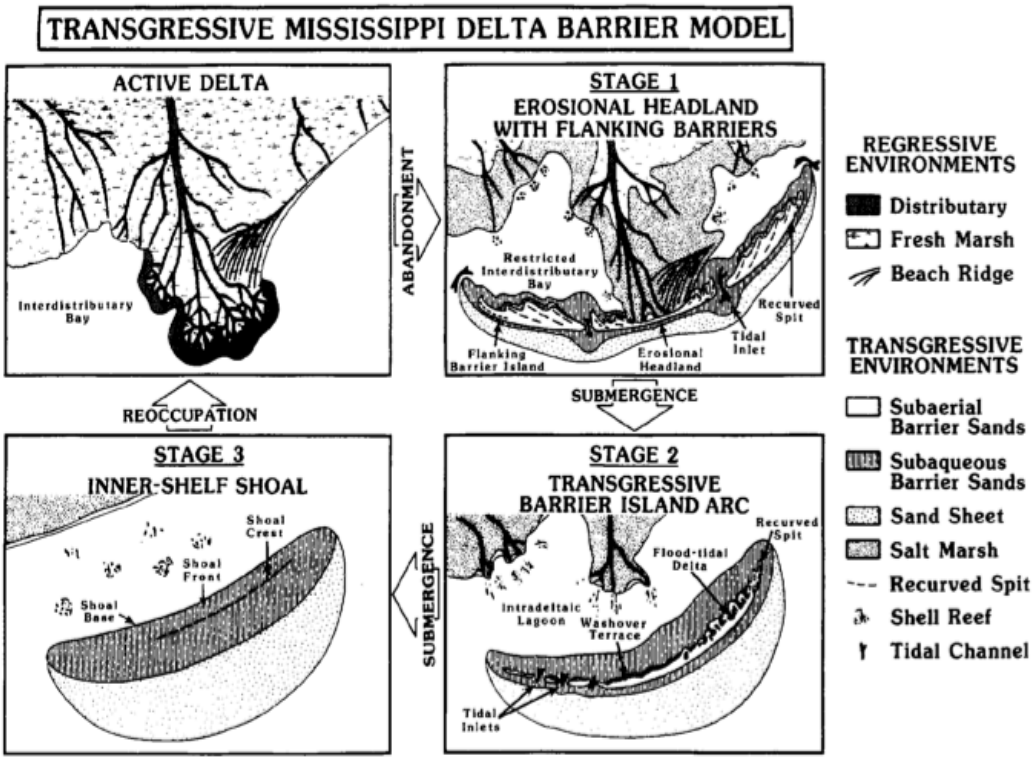

Figure 5: Stages of a transgressive delta and barrier island formation (After Penland, Boyd, and Suter, 1988).

During the transgressive phase of a delta, sediments within distributary channels of the terminated lobe become suspended within the water column and are dispersed laterally via longshore transport processes. Over time, these reworked sands become separated from the mainland, commencing the formation of barrier islands. Further submergence of the headland gives rise to an intradeltaic lagoon and a barrier island fully separated from the terminated delta (stage 2, Figure 3). As transgression continues, the barrier island releases sediment and becomes dispersed, thus decreasing its overall height and volume. This process continues until the once-barrier island succumbs to subsidence and develops into a submarine shoal. The entire deterioration process takes approximately 2,000 to 4,000 years to complete until another delta forms and overlaps the old lobe (Coleman, 1988). This deterioration and submergence phase is currently taking place on the Lafourche deltaic lobe (Coleman, 1988; Day et al., 2007; Roberts, 1997).

2.2.1 The Lafourche Deltaic Complex

Since the 1930s, there has been significant loss of wetlands along the Mississippi Deltaic Plain. This has been a hot topic of investigation in the scientific community, not only to understand the mechanisms causing land loss, but also to implement effective coastal management plans to mitigate future loss. Although eventual deterioration of deltaic wetlands is inevitable, numerous catalytic agents have worked in conjunction to accelerate this process, including the construction of flood control structures along the Mississippi River, altered wetland hydrology caused by levee development, decreased amounts of suspended material in the

Mississippi River due to dam constructions in river basin, and relative sea-level rise (Day et al., 2000). During the 20th century, the Lafourche deltaic complex has been the most susceptible to wetland subsidence and coastal retreat (Penland and Ramsey, 1990).

The Lafourche channel began its progradation approximately 1000 years ago and took about 700 years to become a major delta lobe when it was then subjected to marine reworking and compaction. During this phase, marine waters from the Gulf of Mexico began to encroach into the previously freshwater marshes of the Lafourche delta. This initiated deterioration of the wetlands.

Presently, the Lafourche delta is a transgressive depositional headland system and consists of a central headland (Caminada-Moreau), a pair of recurved spits, flanking barrier islands, and a barrier island to the east (Grand Isle) (Coleman, 1988). Following abandonment of the Lafourche delta, erosion of this coastal region has supplied sediment for the flanking barrier islands, which front two interdistributary bays (Barataria and Timbalier Bay) (Penland, Boyd, and Suter, 1988). This coastline is a discontinuous mainland beach containing marsh outcroppings and backbarrier lagoons along its seaward face, which have been active repositories for hurricane-induced overwash events (Liu et al., 2010, Naquin et al., 2014). Historical maps display 3 km of shoreline erosion of the Caminada-Moreau headland for the years 1887 to 1978 (an average annual shoreline retreating rate of 29 m/year, Penland, Boyd, and Suter, 1988) and an additional 2 km for the years 1954 to 2009 (Naquin et al., 2014).

2.2.2 Black Mangroves

While long-term palynological data of the lower Lafourche delta are lacking, recent studies have focused on evaluating climate-induced shifts in vegetation within coastal Louisiana during the 20th century. The black mangrove (*Avicennia germinans),* a subtropical halophytic intertidal plant, has been widely recognized as a key indicator of localized climatic warming (Henry and Twilley, 2013; Michot, et al., 2010). These studies have shown a strong correlation between the absence of hard-freezing winters and the expansion of *Avicennia* populations, while Michot et al. (2010) recorded a five-fold increase in black mangroves from 2002 to 2009. Michot et al. (2010) found a distinct distribution in the ages of mangrove colonies and their proximity from the coast. Younger plants were concentrated further inland, while more dense patches of mangroves were abundant near the coast, indicating their northward migration. The transition from *Spartina* (coastal cordgrasses) to *Avicennia* in the lower Lafourche delta near Port Fourchon, LA (29^{o}06'21" N, 90^{o}12'30" W) was recorded in the sedimentary record by Henry and Twilley (2013). These vegetation shifts can be highly significant from an ecological point of view, as biogeochemical and physical parameters of underlying sediment are reflected by the vegetation type (Boudreaux, 2012, Henry and Twilley, 2013). *Avicennia* has shown to be more resistant to erosional processes in comparison to *Spartina* which possesses a less developed root system, thus weaker sediment shear strength (Boudreaux, 2012, Cahoon et al., 2006). While the expansion of the black mangrove is often viewed as a warning indicator to rising sea level and

increased winter temperatures, it may have a positive impact on coastal communities facing rapid subsidence such as the Caminada-Moreau headland and Port Fourchon, LA.

2.3 Hurricanes

Tropical cyclones have been defined as non-frontal, synoptic-scale (200-2,000 km in diameter) low-pressure systems that develop over tropical to subtropical waters and have organized convection systems (Emanuel, 2005). While the terms *tropical cyclone* and *hurricane* are typically used interchangeably, *hurricane* is only used when describing a tropical cyclone located in the Central Pacific, Northeast Pacific, and the North Atlantic that possess maximum sustained surface winds of at least 33 m/s (74 mph) (Emanuel, 2005). Hurricanes are classified based upon their wind speed according to the Saffir-Simpson scale (Table 1) with Category 1 being the weakest and Category 5 representing the strongest storm.

2.3.1 Paleotempestology: Methods and Applications

Paleotempestology, the study of ancient hurricanes, has emerged to the forefront of science in recent decades due to its ability to extend tropical cyclone record beyond the historical period. Commonly used proxies include oxygen isotopic ratios in cave deposits and tree rings, beach ridge formations, microfossil assemblages, and storm deposits in coastal backbarrier lakes and marshes (Liu,

2013). However, according to Liu (2004), the detection of past storm deposits by means of stratigraphic analyses in coastal sediments serves as the most effective tool for reconstructing past hurricane activities in coastal settings. Because the instrumental tropical cyclone record is constrained to the past 150 years, the long-term perspective provided by sedimentary paleotempestology can be used to improve the estimate of return periods of intense hurricanes.

Table 1: Tropical cyclone classification and the Saffir-Simpson hurricane intensity scale.

Saffir-Simpson Hurricane Scale			
Category	Wind (mph)	Pressure (millibars)	Surge (ft)
1	74-95	> 980	4-5
2	96-110	965-979	6-8
3	111-130	945-964	9-12
4	131-155	920-944	13-18
5	> 155	919	> 18
Other Tropical Cyclone Classification			
Tropical Depression	< 38		
Tropical Storm	39-73		
Hurricane	74+		

Since coastal backbarrier lakes and deltaic lowlands are frequently impacted by tropical cyclones and the related sedimentary processes, they function as key repositories for storm-driven morphological changes, with overwash sand layers commonly being used as a proxy for large storm events. The thickness and texture of these deposits have often been used to assess the relative intensity of prehistoric events, with the intensity levels calibrated by comparison with the sedimentary signatures of known historic or modern events (Liu, 2004). These studies have

indicated that repeated hurricane strikes will be marked in coastal sediments by interspersed organic and clastic layers (Figure 4), and that these layers can often be identified by visible inspection, LOI, XRF, and grain size analyses. The thicknesses of clastic layers (grey layers, Figure 4) representative of hurricane strike have been found to rely on multiple parameters such as the proximity of the sampling location to marine reservoir, strength of hurricane, the hurricane's landfall location, and the height of the sand barrier as it would take a stronger hurricane to overtop a high barrier than a low one. In addition to the thickness of the storm deposits found within sediment cores, the overall shape and direction of the overwash fan is dependent on the strength of the hurricane and its direction upon landfall (Figure 5).

2.3.2 Hurricane History of South Louisiana

The Atlantic Ocean is the world's 3rd most active basin in terms of tropical cyclone activity (HURDAT, 2014). Typically, hurricanes that affect this region develop in the eastern portion of the tropical Atlantic Ocean and travel westward toward North America. Studies have suggested that climatic conditions such as the North Atlantic Oscillation (NAO) produce a steering mechanism that controls the location of hurricane landfall (Elsner et al., 2000). The Bermuda High hypothesis, proposed by Liu and Fearn (2000), postulates that long-term shifts in the position of the Bermuda High lead to anti-phase activity patterns between the Gulf of Mexico coastline and the Atlantic coast of the United States.

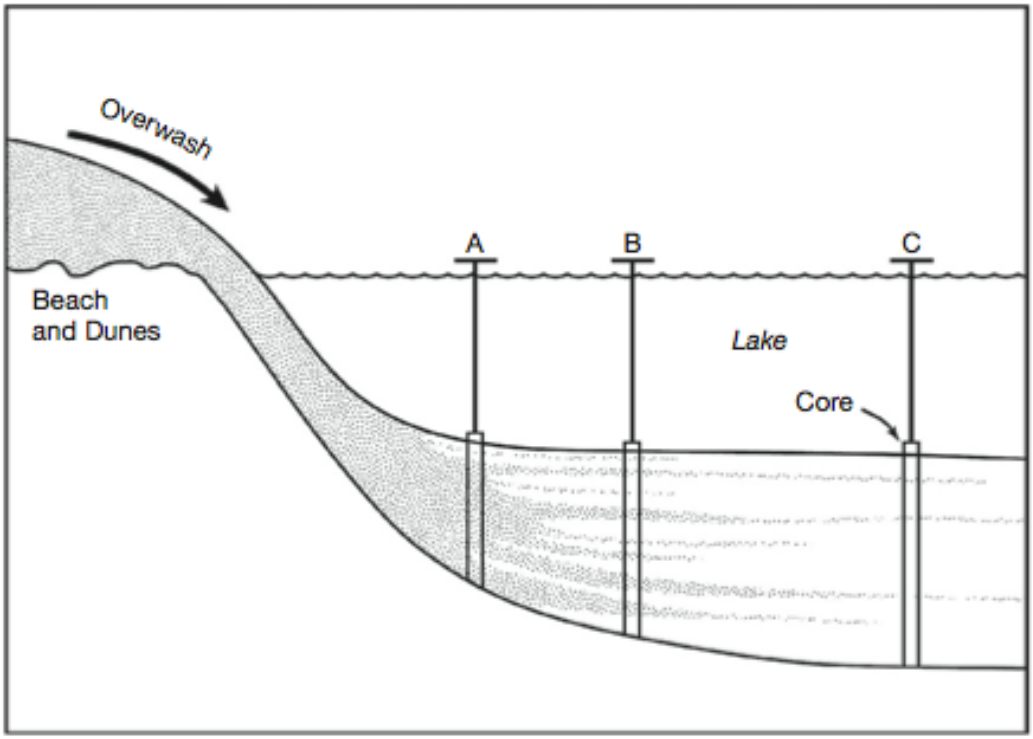

Figure 6: Diagram illustrating long-term preservation of hurricane overwash events (grey layers) into a backbarrier lake. Thickness and texture of sediments in hurricane layers are dependent on distance from the barrier. After Liu (2004).

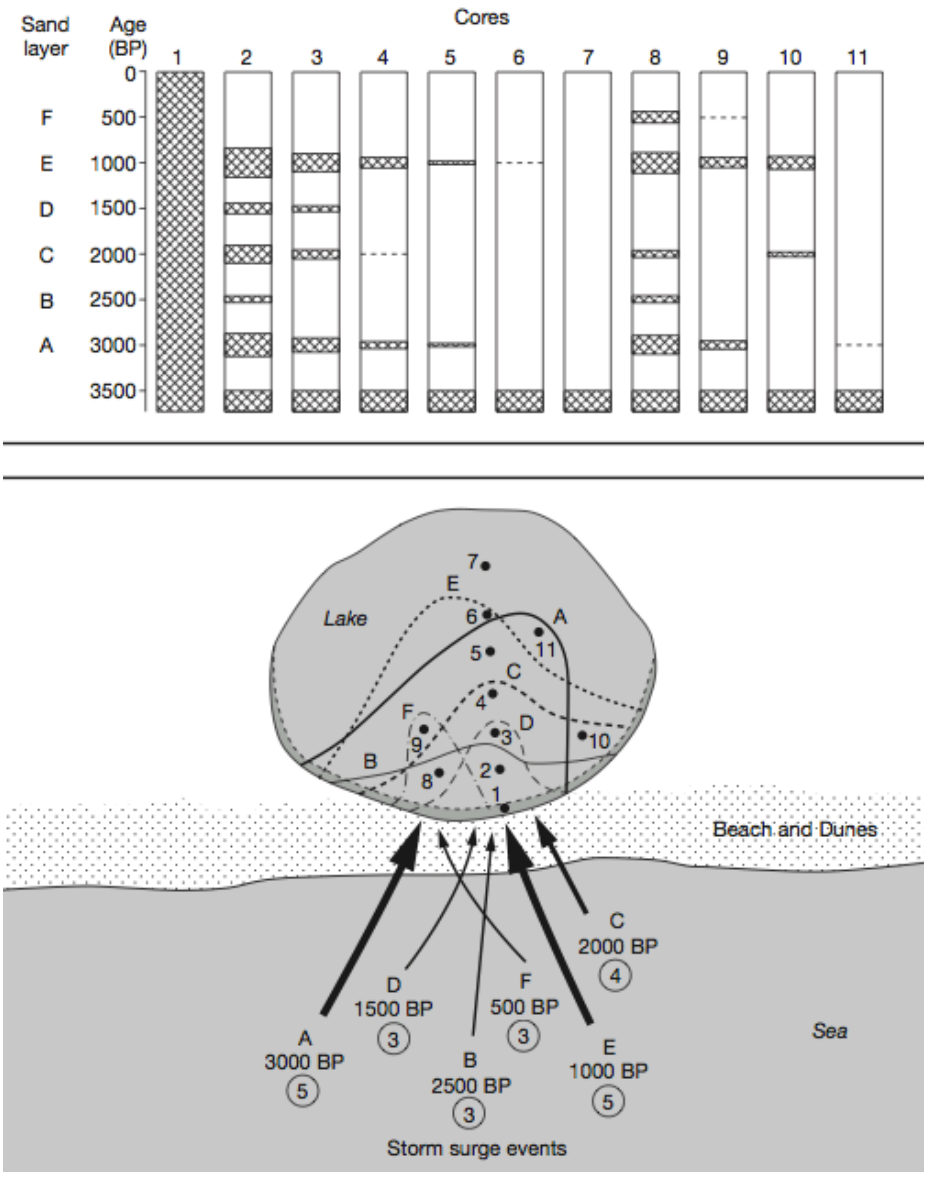

Figure 7: Illustration displaying how the hurricane intensity and its positioning along a coastline affect the shape of an overwash fan and the amount of sediment displaced into a backbarrier reservoir (After Liu, 2013).

Historical and instrumental records indicate that south Louisiana has been highly susceptible to hurricane influence during the past 200 years and the earliest record of large tropical cyclones was in 1527. Historical documents reveal that on October 23, 1527 a large storm affected voyager Panfilo de Narvaez and his crew of roughly 250 men while in search of the Mississippi River (NOAA, 2014). The first well-documented hurricane to strike Louisiana was on September 22, 1722. It was reported that "winds of hurricane force lasted fifteen hours at 10 PM on the 22nd and ending shortly after noon on the 23rd." Storm surges were up to three feet at Bayou St. John and at eight feet in the Mississippi River. Thirty-six homes and the local hospital were destroyed in New Orleans. This storm was even responsible for the moving of Mobile, AL from 27 miles South the mouth of the Mobile River to its current location. Instrumental records supplied by the National Oceanic and Atmospheric Administration's Coastal Services Center show Louisiana's high exposure to hurricane activity (Figure 6).

2.3.3 Hurricane Isaac

Hurricane Isaac (21 August-3 September 2012) made its first landfall along the coast of southeastern Louisiana as a Category 1 hurricane around 0000 UTC 29 August (Berg, 2013). According to the National Hurricane Center (2013), Hurricane Isaac possessed maximum sustained winds of 70 kt at initial landfall then the storm's center diverted westward back over water before making a second landfall directly west of Port Fourchon, Louisiana, around 0800 UTC 29 August (Figure 7). It is reported that the storm slowed down upon its secondary landfall, which allowed

Isaac to strengthen its winds, storm surge, and precipitation. Tide gauges from Grand Isle meteorological station (GISL1-8761724; 29.26 °N, 89.96 °W), just 7 miles east of Port Fourchon, recorded a maximum wind gust of 74 kt and storm surge of 1.3 m (Berg, 2013).

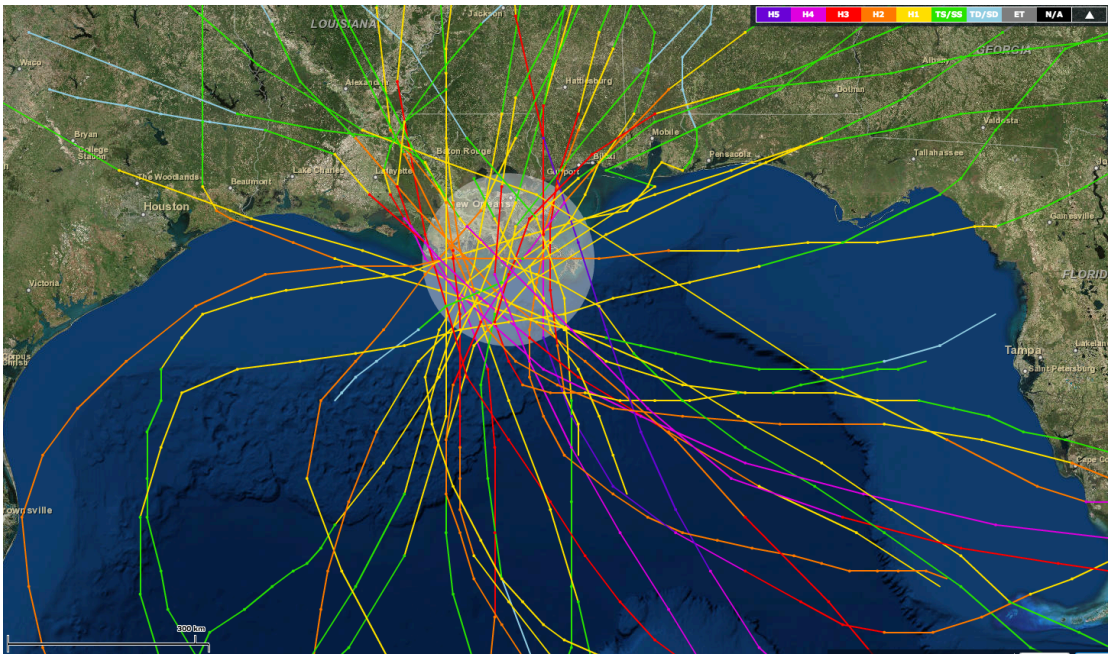

Figure 8: Past hurricane track record of landfalling hurricanes within 65 nautical miles of Port Fourchon, LA (HURDAT, CSC, 2014).

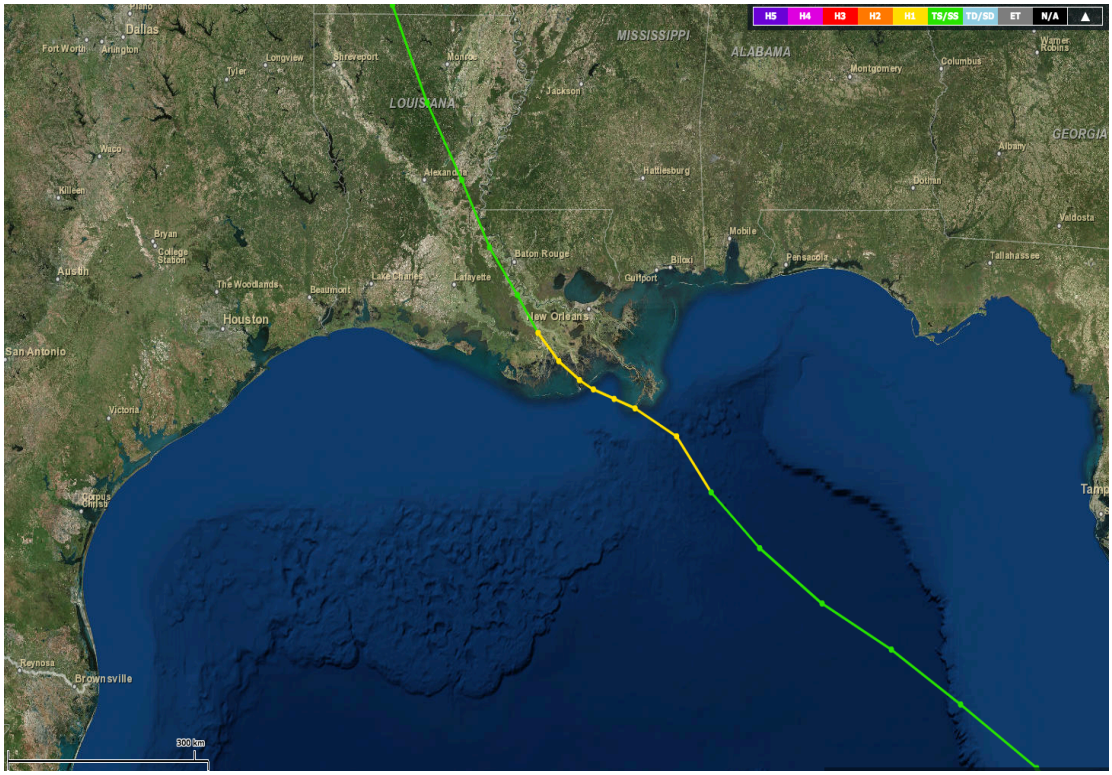

Figure 9: Path of Hurricane Isaac (September, 2012) (HURDAT, CSC, 2014).

CHAPTER 3. STUDY SITE

3.1 Coastal Environment and Vegetation Communities

The Caminada-Moreau coastline of Louisiana is a Chenier system consisting of marshlands, backbarrier lagoons, and a barrier island. This complex has been reworked by marine processes since the termination of the Lafourche distributary system approximately 600 years ago (Day et al., 2007; Penland et al., 2005; Penland and Ritchie, 1979). The geomorphological causes to this include beach face erosion, littoral drift, hurricane washover events, and aeolian sand transport (Penland and Ritchie, 1979). These processes in combination with insufficient amounts of riverine sediments have led to an increase in marine influence to the area as early as the 1700s (Day et al., 2007; Penland and Ritchie, 1979). Salinities in this region average 20-22 $^{0}/_{00}$ in estuarine locations (Bayou Lafourche, Caminada Bay) and reach up to 30 $^{0}/_{00}$ near the boundary between Bayou Lafourche and the Gulf of Mexico. Average temperatures range between 16^{o}C in January to 32^{o}C in August (Brown and Swearingen, 1998). These climatic and hydrological factors play a direct role in shaping the local vegetation. Historical accounts document that the easternmost barrier island (Grand Isle) of the Caminada-Moreau complex existed as a Chenier populated by live oaks until the 1780s, when this region was deforested to suit cotton and sugar cane agricultural practices (Cowan et al., 1983). In recent decades, vegetation records have shown that the Caminada-Moreau system is dominated by a mix of polyhaline and mesohaline marsh herbaceous taxa such as Amaranthaceae and *Typha* (Visser et al., 1998); however, the recent introduction

and expansion of *Avicennia germinans* (black mangrove) has also been documented (Henry and Twilley, 2013). Currently, both herbaceous taxa and *Avicennia germinans* appear to be of equal abundance. This region is the northernmost boundary in which *Avicennia germinans* are found, and it exists in the dwarf shrub growth form (Henry and Twilley, 2013). Black mangroves are most common flanking large bays in the lowermost regions of Bayou Lafourche, near Port Fourchon.

3.2 Port Fourchon, Louisiana

Located on the southern tip of Lafourche Parish, Louisiana is the state's southernmost port, Port Fourchon. It is situated directly northwest of the Caminada-Moreau headland and utilizes Bayou Lafourche as a gateway to the Gulf of Mexico for industrial commerce and recreational and commercial fisheries. Port Fourchon was formally established in 1963 by the Greater Lafourche Port Commission and since then it has become one of the United States' most lucrative ports (GPLC, 2009). A 30-year projection expects Port Fourchon to cater to nearly 60% of all natural gas and oil exploration off the coasts of Louisiana, Mississippi, and Alabama (Brewton et al., 2009). This area is not only vital to the success of nearby local economies, but also for the nation's international fisheries and petroleum trade. However, continued expansion of this region could lead to further compaction of land in this sediment-starved regime, thus providing an additional catalyst to local subsidence. Our study site, Bay Champagne, serves as an active

repository in recording geologic changes created by tropical cyclones in the area as well as long-term vegetation changes due to environmental stress.

3.3 Bay Champagne

Bay Champagne, a semi-circular, shallow (<1 m) backbarrier lagoon situated along the Caminada-Moreau headland, is positioned on a WSW to ENE axis on the seaward margin of the Lafourche deltaic lobe near Port Fourchon, Louisiana (Figure 8). As early as the 1950s, Bay Champagne existed as a fully-circular body of water, enclosed by marshland. Since then, the coastline has rapidly retreated inland (Henry and Twilley, 2013; Naquin et al., 2014). Subjected to annual subsidence rates of 1-1.2 cm $year^{-1}$, Bay Champagne is currently much reduced in size, thus developing a semi-circular shape (Figure 9). The lagoon receives water input from fresh and salt-water sources and is separated from the Gulf of Mexico by a 1 m high sand barrier. This barrier prevents marine waters from entering the bay during normal tidal processes, although it cannot prevent marine inundation during storm surge events generated by major hurricanes (Liu et al., 2011; Naquin et al., 2014).

Figure 10: Aerial photograph of Port Fourchon (outlined in white) and Bay Champagne (white arrow). Image modified after Google Earth (2008).

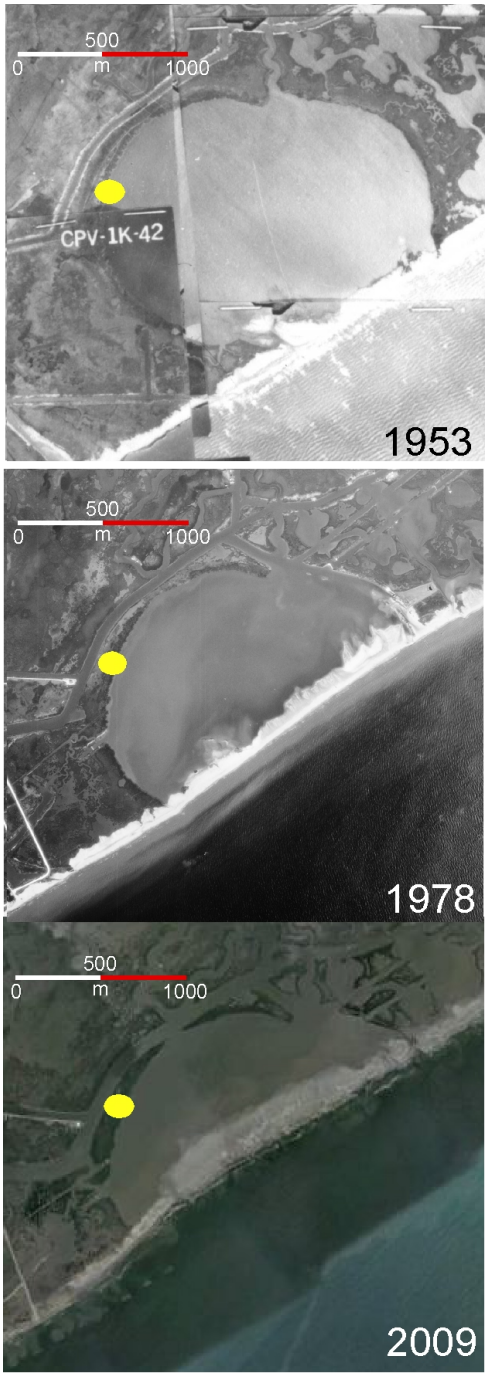

Figure 11: Satellite images displaying coastal transgression occurring in the Port Fourchon, Bay Champagne area between 1953 and 2009. Coring site of BC53 is denoted by the yellow dot. Images courtesy of the Louisiana State University Map Library. Modified after Naquin et al. (2014).

CHAPTER 4. METHODOLOGY

4.1 Field Work

On September 21, 2012, two weeks after the impact of Hurricane Isaac, a 2.2 m core (BC53) was extracted from a small pond surrounded by saltmarsh located in a narrow strip of land on the northwestern shore of Bay Champagne near Port Fourchon, LA (29°07'N, 90°10'W) (Figure 9). The core was taken to provide material for a study to reconstruct paleoenvironmental changes and geologic signatures left by tropical cyclones. After marking the coring site by using a handheld GPS device, sediment was collected using a 3-inch inner-diameter (ID) aluminum vibra-core tube. Core BC53 was capped, sealed with tape, and transported to Louisiana State University in Baton Rouge, LA where it was preserved in a cold room at 4^{o}C.

4.2 Laboratory Work

Core BC53 was extensively analyzed in the Department of Oceanography and Coastal Science's Global Change and Coastal Paleoecology Laboratory and Marine Geochemistry Laboratory at Louisiana State University. The 2.2 m sediment core was divided into two equal-length sections and cut in half longitudinally using an electrical rotary saw.

4.2.1 Geochemical Analyses

The core was opened, examined for physical changes, described by using a standard Munsell soil color chart, and photographed using a digital camera. Loss-on-ignition (LOI) analysis was performed at 1 cm continuous intervals following the

method described by Liu and Fearn (2000). Stratigraphic profiles of 26 chemical elements were determined by using a Delta Innov-X handheld X-ray fluorescence device. Core BC53 was covered with a plastic wrapping to prevent contamination, then subjected to three 15-second intervals of X-ray bombardment at 40-kV excitation at continuous 2 cm intervals. Of the 26 elemental profiles that were yielded, 9 were selected (Br, Cl, Co, K, Rb, S, Sr, Ti, and Zn) for display and interpretation due to their significance in this study.

Loss-on-ignition and X-ray fluorescence (XRF) analyses allow the determination of sediment type and origin while also being used to infer environmental changes. More importantly, they assist in identifying hurricane-induced deposition that cannot be detected by the naked eyes.

4.2.2 Pollen Analysis

Palynological data in the upper meter of the core were obtained by extracting 1 mL of sediment at approximately 10 cm intervals. Pollen and microscopic charcoal were examined to determine vegetation change within the area and the presence of fire or drought, respectively. Standard pollen extraction techniques were performed according to Faegri and Iversen (1989) with the addition of a marker tablet containing approximately 1.8×10^4 *Lycopodium* spores, used to determine pollen concentration and influx. Chemical treatment began with the addition of 10% HCl to break down carbonate compounds found within the sample, followed by 10% KOH treatment in a hot water bath to remove humid acids. This was followed by centrifuging, decanting, and washing samples with deionized

water. These steps were repeated until the supernatant appeared colorless, indicating that most humic acids had been removed from the sediment. Cold HF (70%) was then added to eliminate any silicates. Following decanting the excess HF and washing the sample with water, glacial acetic acid (GA) was added to wash the sediment, eliminate any water, and slightly acidify the sample. An acetolysis solution was prepared separately by applying 9 parts acetic anhydride to 1 part concentrated sulfuric acid. After preparing the acetolysis solution, it was applied to each test tube while being heated in a boiling water bath for approximately 2 minutes. This process ensures that all cellulose within the sample is dissolved. Cellulose dissolution is followed by repetitive washing with GA, centrifuging, and decanting excess waste. The remaining sediment sample was transferred to a labeled vial and stirred to ensure homogeneity while adding 2-3 mL of tertiary butyl alcohol (TBA). Approximately 2 mL of silicone oil was added as a mounting medium. Vials were stored uncapped overnight to allow evaporation of excess TBA. Pollen and charcoal counts were achieved by using a Motic BA200 microscope at 40x magnification. Twenty-four samples were observed until at least 300 pollen grains were counted in each. Identification was aided with regional pollen keys by McAndrews et al. (1973) and Willard et al. (2004).

Overall, pollen was well preserved and showed minimal signs of degradation. Ten (10) taxa were identified within core BC53 and were grouped according to vegetation type. Pollen counts are displayed in percentages based on a sum of all pollen and spore taxa, with the exception of dinoflagellates and foraminifers in

which raw counts are shown. Pollen concentration is expressed as grains per unit volume (cc) and charcoal concentration as fragments per cc. An indeterminable pollen curve is included in the diagram, as these are grains that were corroded or degraded beyond identification.

4.2.3 Isotopic and Radiocarbon Dating Analysis

During the 1950s, atomic bomb testing led to the injection of radioactive isotopes into the atmosphere. The fallout of ^{137}Cs and other isotopes in the ^{238}U decay chain allows soil particles to rapidly flocculate to them upon their arrival to Earth's surface. ^{137}Cs is among one of the more widely used tracers for studying erosion, sedimentation rates, and establishing a chronological marker within the stratigraphy as there is a direct correlation with the peak within a Cs profile and the termination of nuclear device testing. Since the known maximum fallout flux of Cs occurred before 1963, the annual deposition rate since the ban of nuclear arms testing can be calculated in undisturbed sedimentary environments as described by the following equation:

$$R = \frac{H}{n - 1963}$$

where *R* is the deposition rate (cm/year), *H* is the depth of the peak in Cs activity (cm), and *n* is the sampling year (Bai, Zhang, and Wang, 2011).

To determine isotopic profiles of ^{137}Cs, 10 sediment samples weighing approximately 10 g (wet weight) each were subsampled from the core and dried in ceramic crucibles at 100^{o}C for 24 hours. Then samples were grinded to a consistent powder-like material by using a pestle and mortar, compacted into plastic vials, and

covered with an epoxy resin to prevent isotopic decay within the vial. Samples were analyzed by using a well calibrated gamma spectrometry using a hyper pure coaxial germanium detector and multichannel analyzer system. ^{137}Cs peak was measured at 661 keV energy.

4.2.4 Radiocarbon Dating

Charcoal and wood fragments were extracted from BC53 at three depths (80, 123, and 224 cm) for Accelerator Mass Spectrometry (AMS) radiocarbon dating to develop a long-term age profile of the core. Samples were sent to the National Ocean Sciences AMS laboratory at Woods Hole Oceanographic Institution in Massachusetts, USA for radiocarbon analysis. Radiocarbon dates received were converted to calendar years by using the Calib 7.0 program developed by Stuvier and Reimer (2005).

4.2.5 Dry Extraction

Three bulk sediment samples A1 (5 cm depth), A2 (6 cm) and A3 (7 cm) were removed from BC53 and subjected to a dry extraction analysis to determine crude oil contamination of the coring site. An amended version of the United States Environmental Protection Agency method 3550B was performed by Laura Basirico in the Marine Ecotoxicology Lab in the Department of Oceanography and Coastal Sciences at LSU. Samples were freeze-dried, treated with a dichoromethane solvent, and sonicated to break down cell matrices attached to potentially contaminated sediments. Supernatant was decanted. The solvent-sonication process was repeated three times to ensure that all contaminants were extracted

from sediments. Following this, samples were filtered and subjected to evaporation. Hexane was then added as an injection solvent. Samples were analyzed by using a Hewlett Packard 5890 Gas Chromatogram Mass Spectroscopy instrument. Analysis was performed in selective ion mode (SIM) to quantitate alkane and aromatic constituents. Six standards were used during investigation. Four internal reference standards (Napthalene-d8, Acenapthalene-d10, Chrysene-d12, and Perylene-d12) were used to calculate concentration while two standards were used to calculate alkane and aromatics recovery (5-alpha androstene and Phenanthrene d-10). Alkane values were reported in µg/g while aromatic compounds were recorded in ng/g. Surrogate values were established to calculate recovery efficiency of constituent compounds.

CHAPTER 5. RESULTS

5.1 Lithology

Loss-on-ignition (LOI) data and visual inspection suggest three distinct stratigraphic zones within Core BC53 (Figure 10). Sediments are described based on texture and LOI data. Zone I (222-142 cm depth range) contains light grey mud interspersed with reddish brown laminations occurring at 0.5-1.0 cm intervals. This zone is marked by fairly uniform LOI results as noted by 45 to 50% water content, 10% organics, and 5% carbonate with the exception of an approximately 8% spike in carbonate at 143 cm. Zone II (141-102 cm), a much more dynamic zone, is noted by an abrupt change to grey mud which is interrupted by a fragmented peaty mud layer (138-130 cm) positioned above fine sand. Above this layer is grey mud, which is defined by a 25% decrease in water content. The peat layer occurring at 117-110 cm is marked by a 20% increase in organics as well as a 25% increase in water content. Zone III (101-0 cm) is represented by alternating grey mud and brown peaty mud layers. Zone III contains fairly uniform LOI data with the exception of two layers of higher organic contents (27-20 cm, 10-3 cm) alternating with two layers of higher clastic contents (20-12 and 2-0 cm) near the top. ^{137}Cs analysis was performed within this zone with a prominent activity peak found at 27 cm (Figure 11). A dark band at 5-10 cm marked by a 15% increase in LOI values is attributed to the presence of crude oil (Table 2).

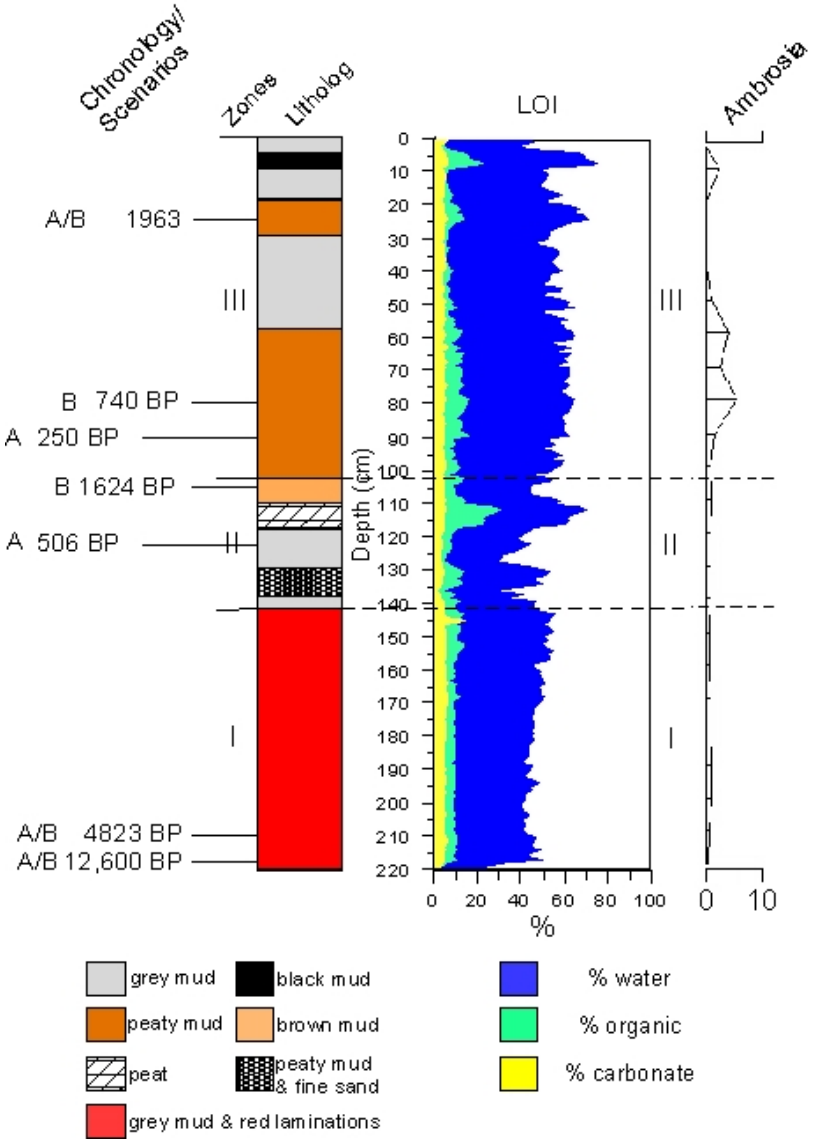

Figure 12: LOI and litholog diagram of Core BC53. Radiocarbon dates are shown in conventional values before calibration.

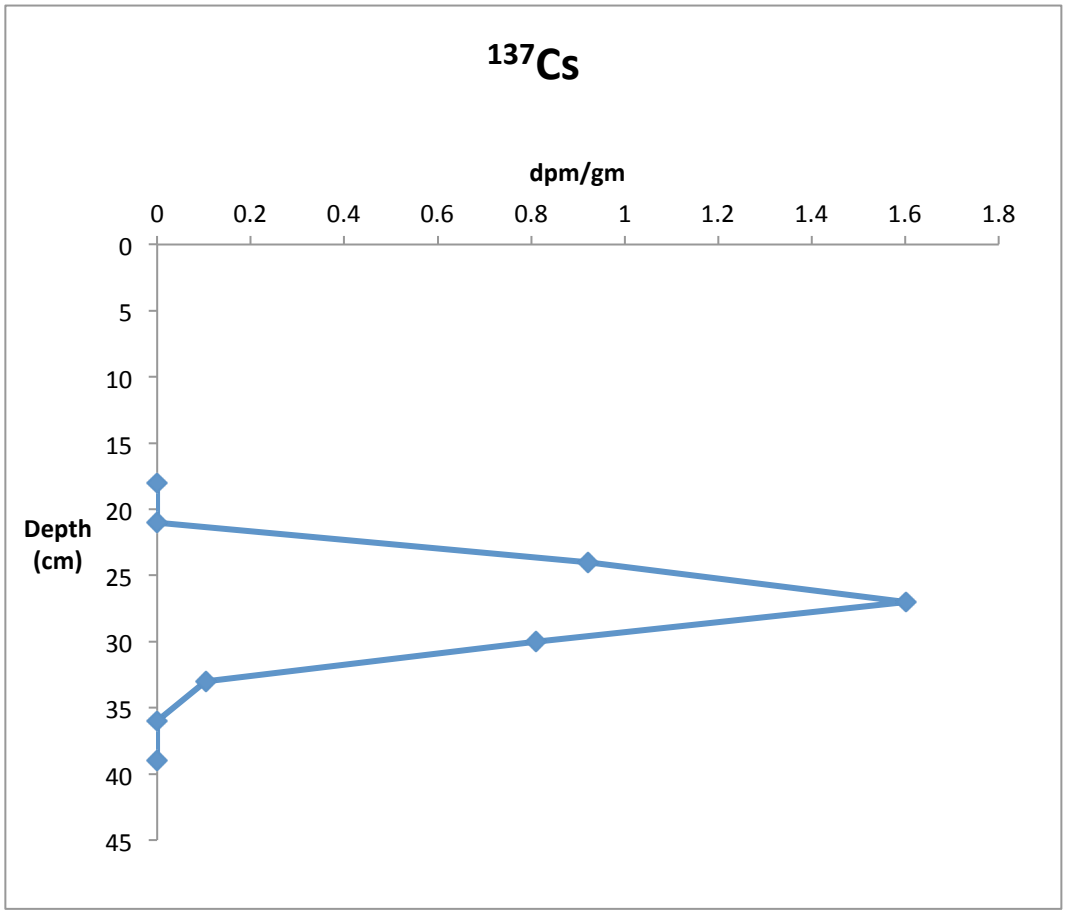

Figure 13: ^{137}Cs profile of Core BC53.

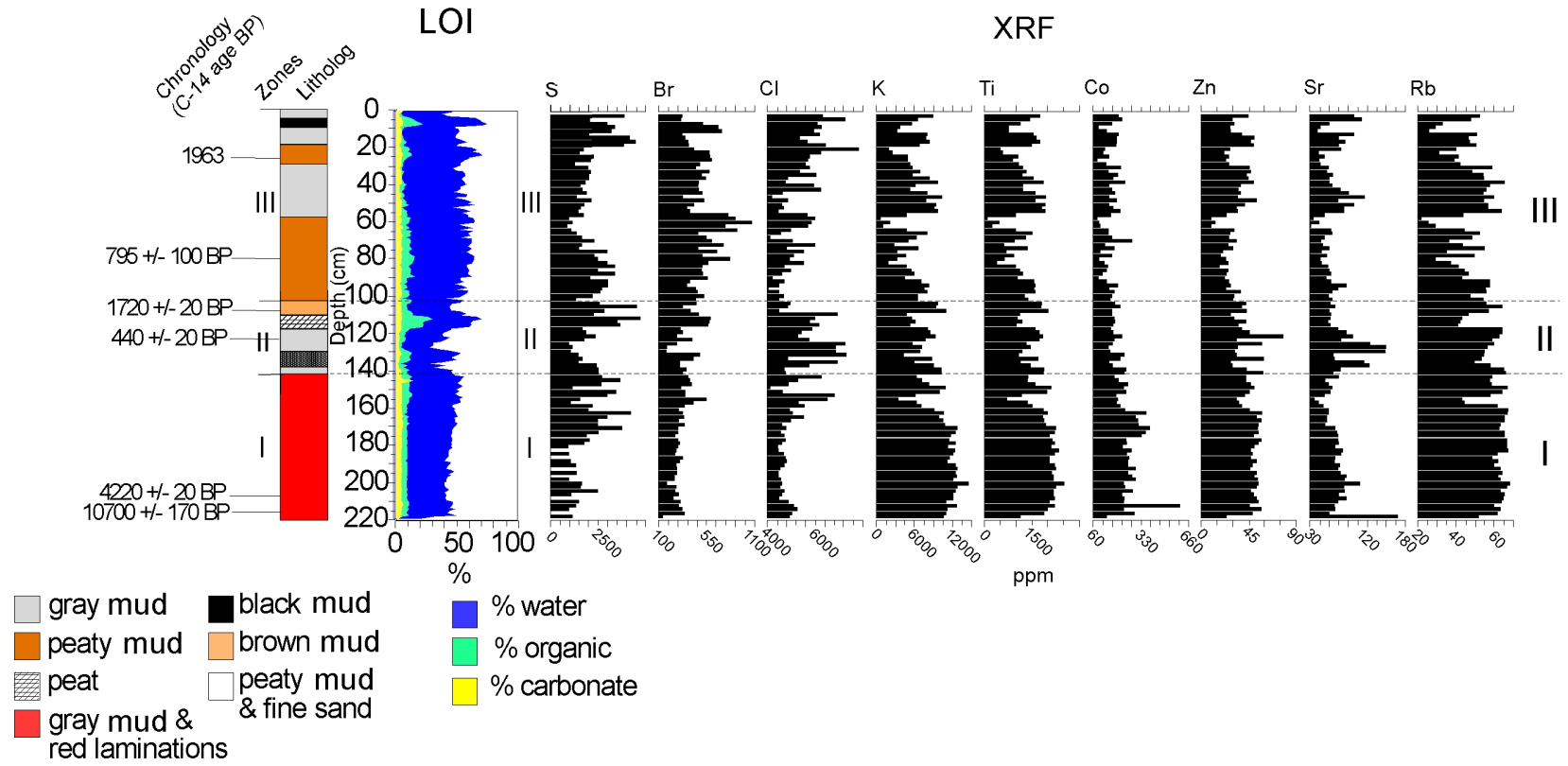

Figure 14: XRF, LOI, and litholog data of Core BC53.

5.2 X-ray Fluorescence

X-ray fluorescence established elemental profiles of Br, Cl, Co, K, Rb, S, Sr, Ti, and Zn within the core (Figure 12). Transition metals (K, Ti, Co, Zn, and Sr) and alkali metal Rb show a near-parallel relationship. These elements display uniform concentration curves within Zone I (142-219 cm), followed by an overall decrease upward, with exceptions found in the grey mud layers in Zone III (0-2, 12-20, and 28-55 cm) and in Zone II (103-110 and 116-130 cm) in which there were significant increases in elemental contents. The halogen elements (Br and Cl) show an anti-phase existence with the transition metal group. The Cl/Br ratio exhibited a maximum at 131-123 cm while also displaying large spikes at 20-10 cm and 3-0 cm (Figure 13). S showed a unique sequence in contrast to the other elements of interest. This profile expresses large increases at various depths within the core. These increases are present in Zone III (8-20 cm), Zone II (102-112 cm) and Zone I (150-155, 160-165, and 170-178 cm).

5.3 Palynology

Twenty-three (23) total samples were extracted for pollen analysis. The pollen diagram is shown in Figure 14. Pictures of important pollen taxa are found in Figure 15. Herbaceous pollen taxa (Poaceae, Amaranthaceae, and *Typha*) dominate throughout the core while arboreal taxa *Pinus* and *Quercus* displayed low to moderate values (5-20%) and *Quercus* showed low percentages (<3%). Other local taxa generally have lower percentages. Notable among these pollen taxa is *Avicennia germinans*, which is confined to the upper 56 cm of Core BC53. Charcoal concentration is relatively low in Zone I

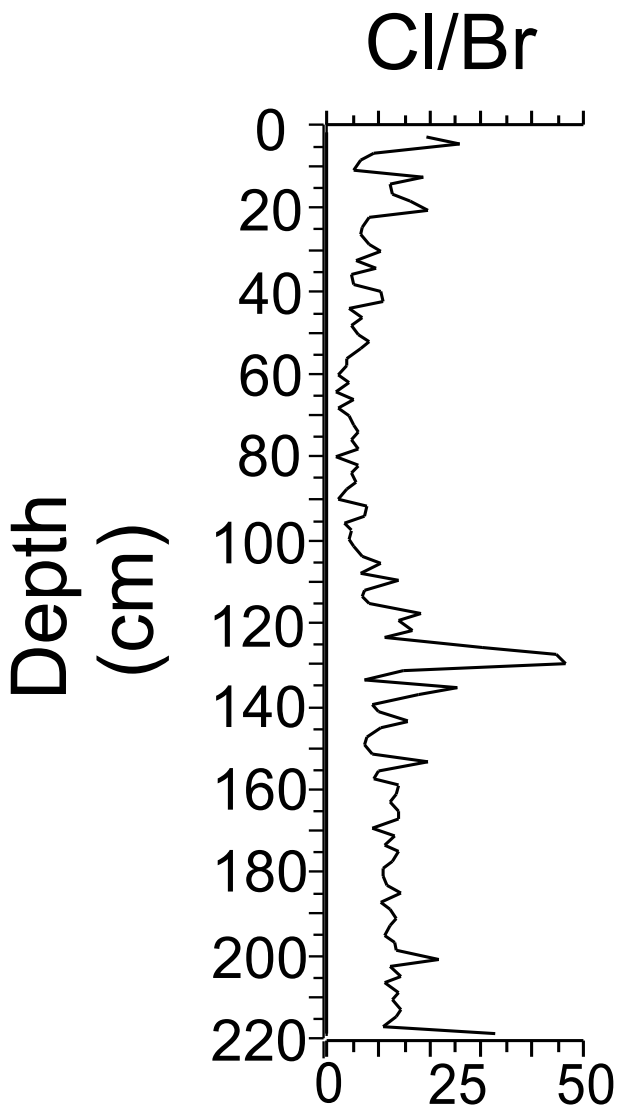

Figure 15: Cl/Br ratio derived from XRF analysis.

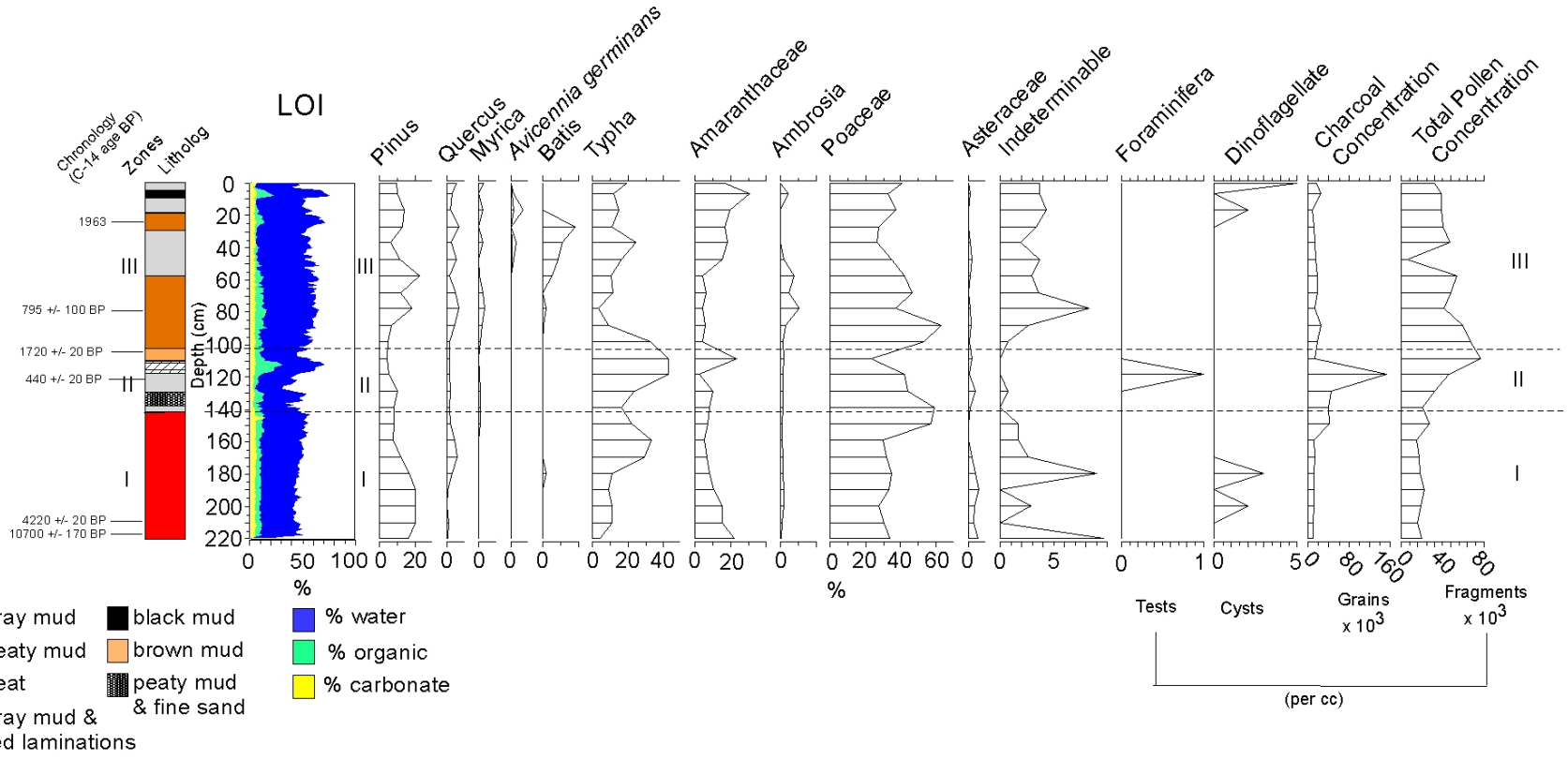

Figure 16: Pollen diagram combined with LOI and litholog data of Core BC53.

but increases sharply in Zone II, culminating in a large spike near the middle depths (116 cm) of the core.

5.3.1 Zone I

Zone I consists of 8 samples. *Pinus* and Amaranthaceae percentages display gradual decreases throughout the zone. Poaceae percentages remain fairly constant with an increase from 25 to 58% at the Zone 1-Zone II boundary while *Typha* ranged from 5 to 35% throughout the zone. Two samples (176, 196 cm) contained dinoflagellates. Charcoal concentration was minimal with the exception of a 3-fold increase at the uppermost sample taken from Zone I.

5.3.2 Zone II

Zone II contains 4 samples. This zone is characterized by maximum percentages of *Typha* and low arboreal taxa composition (*Pinus*, 5-10%; *Quercus*, <3%). Total pollen concentration increases to maximum values in this zone. Among other herbaceous taxa, *Poaceae* gradually decreases, while Amaranthaceae shows a spike at the top of the zone. One foraminifera test was found just below the peat layer in this zone. In addition, charcoal concentration increases to a prominent peak at the same depth in which the foraminifera was found.

5.3.3 Zone III

Zone III consists of 11 pollen samples. This zone is marked by an overall increase in *Pinus* and *Quercus* in comparison to the other two zones. *Batis* displayed a secular increase (5-20%) from 66-36 cm. *Amaranthaceae* showed an overall increase while *Typha* and *Poaceae* contained moderate to high

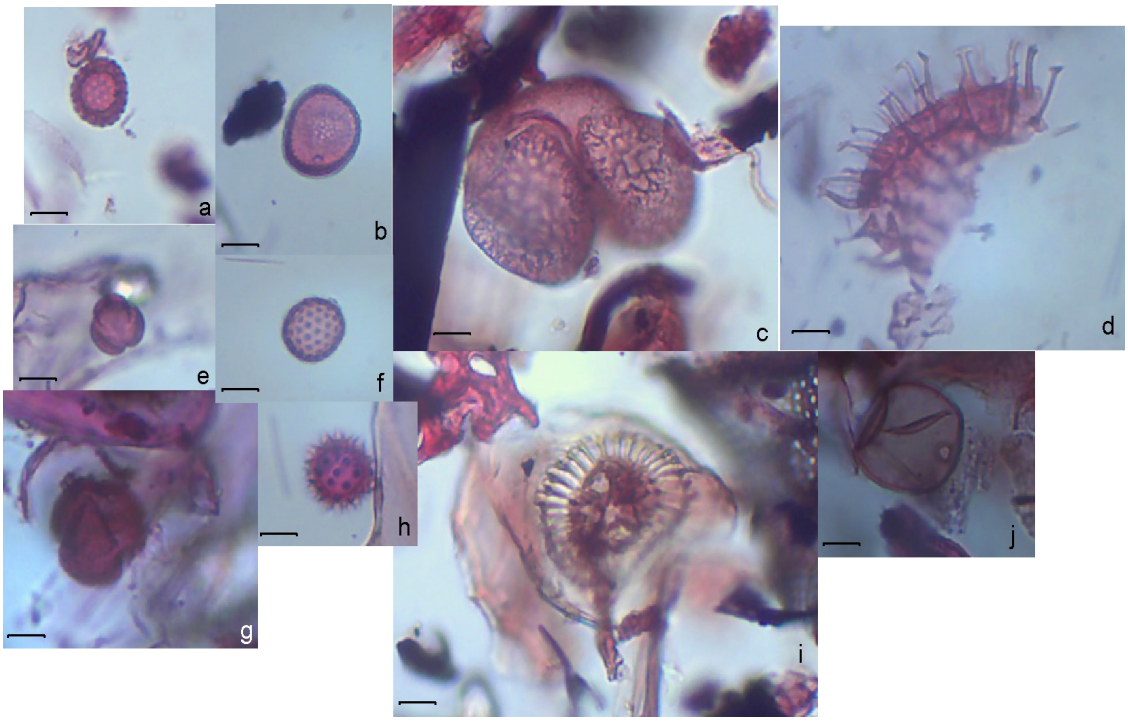

Figure 17: Important pollen taxa found in Core BC53. a: Ambrosia; b: Typha; c: Pinus; d: dinoflagellate; e: Batis; f: Amaranthaceae; g: Avicennia germinans; h: Asteraceae; l: foraminifera test; j: Poaceae. Scale bars: 10 µm.

concentrations throughout the depths within this zone. *Ambrosia* exhibited a significant increase from 86-66 cm. *Avicennia germinans* appeared within the stratigraphy at 56 cm and displayed a maximum at 26 cm. The highest concentration of dinoflagellates was found within the upper depths of Zone I in which there were 2 found at 26 cm and 5 found at 6 cm.

5.4 Core Chronology

5.4.1 Crude Oil Marker Horizon

Dry extraction analysis of three bulk sediment samples taken from a dark sediment band (4-10 cm) found within BC53 gave rise to the presence of crude oil constituents (Table 2). Total mean concentration of alkanes and aromatic compounds are 30.74 µg/g and 25,990 ng/g, respectively. Surrogate recovery percentages were over 50% for all samples. Total ion chromatograms (TIC) for samples A1 (Figure 16), A2 (Figure 17), and A3 (Figure 18) were compared to the MC252 source chromatogram (Figure 19). There was no definitive correlation between samples analyzed and MC252 source crude oil.

5.4.2 ^{137}Cs Profile

^{137}Cs was found in four of the 10 samples analyzed. Depth distributions of ^{137}Cs are shown in Figure 11. A well-defined peak was found in the profile at 27 cm, indicating the year 1963 horizon. The position of this peak within the stratigraphy suggests an approximate average sedimentation rate of 0.55 cm/year on the top 27 cm of Core BC53.

5.4.3 Radiocarbon dating

Radiocarbon dating in conjunction with ^{137}Cs analysis presents two scenarios regarding the depositional history of the BC53 coring site. These radiocarbon ages and calibrated dates are displayed in Table 4. Two radiocarbon samples (80 cm and 106 cm, Table 4) appear to be out of sequence within the stratigraphy. For a detailed argument regarding establishing a reliable age model, see Chapter 6.

Table 2: Alkane concentrations for all samples in dry extraction analysis.

Sample ID	A1	A2	A3
Units	ug/g	ug/g	ug/g
nC-10 Decane	0.037	0.026	0.023
nC-11 Undecane	0.048	0.031	0.021
nC-12 Dodecane	0.034	0.022	0.016
nC-13 Tridecane	0.034	0.021	0.014
nC-14 Tetradecane	0.065	0.036	0.022
nC-15 Pentadecane	1.725	1.056	0.660
nC-16 Hexadecane	0.155	0.107	0.086
nC-17 Heptadecane	3.373	2.350	1.589
Pristane	0.914	0.558	0.374
nC-18 Octadecane	1.162	0.764	0.629
Phytane	0.565	0.352	0.266
nC-19 Nonadecane	0.640	0.410	0.308
nC-20 Eicosane	0.468	0.275	0.190
nC-21 Heneicosane	0.657	0.458	0.326
nC-22 Docosane	0.421	0.294	0.229
nC-23 Tricosane	0.339	0.328	0.292
nC-24 Tetracosane	0.374	0.410	0.437
nC-25 Pentacosane	0.462	0.528	0.608
nC-26 Hexacosane	0.314	0.319	0.368
nC-27 Heptacosane	0.854	0.979	1.067
nC-28 Octacosane	0.291	0.274	0.342
nC-29 Nonacosane	1.044	1.244	1.204
nC-30 Triacontane	0.441	0.469	0.558
nC-31 Hentriacontane	1.707	2.151	2.128
nC-32 Dotriacontane	0.304	0.315	0.372
nC-33 Tritriacontane	0.775	0.996	0.986
nC-34 Tetratriacontane	0.169	0.155	0.186
nC-35 Pentatriacontane	0.224	0.300	0.304
Total Alkanes	**17.59**	**15.23**	**13.61**
Surrogate Recovery (%)			
5 Alpha Androstane	56	54	56

Table 3: Concentrations of aromatic compounds of all samples in dry extraction analysis.

Sample ID Units	A1 ng/g	A2 ng/g	A3 ng/g
Naphthalene	204.303	217.948	222.190
C1-Naphthalenes	323.216	315.696	317.449
C2-Naphthalenes	376.133	330.199	337.269
C3-Naphthalenes	344.225	235.690	208.220
C1-Dibenzothiophenes	760.637	433.338	277.951
C2-Dibenzothiophenes	1518.183	866.233	553.442
C3- Dibenzothiophenes	1189.034	703.098	436.799
Phenanthrene	2692.313	1648.047	2089.603
C1-Phenanthrenes	924.165	523.799	366.714
C2-Phenanthrenes	1252.033	721.445	457.420
C3-Phenanthrenes	1178.480	659.397	412.140
Pyrene	313.806	159.971	120.960
C1- Pyrenes	145.593	77.876	51.570
C2- Pyrenes	52.183	26.804	19.510
C3- Pyrenes	12.583	7.539	8.215
C4- Pyrenes	5.620	4.361	5.558
Benzo (a) Anthracene	6.863	2.144	2.456
Chrysene	13.128	6.002	5.139
C1- Chrysenes	9.124	5.323	6.128
C2- Chrysenes	7.010	7.377	9.299
C3- Chrysenes	4.445	4.497	5.519
C4- Chrysenes	5.125	5.137	5.024
Benzo (b) Fluoranthene	20.003	12.128	10.137
Benzo (k) Fluoranthene	6.324	4.221	7.526
Benzo (e) Pyrene	8.010	3.618	3.974
Benzo (a) Pyrene	6.528	2.424	2.847
Perylene	25.240	22.811	23.505
Indeno (1,2,3 - cd) Pyrene	6.184	2.760	3.437
Dibenzo (a,h) anthracene	1.435	0.497	0.628
Benzo (g,h,i) perylene	5.143	2.350	2.361
Total Aromatics	**17,112**	**10,973**	**9,862**
% Surrogate Recovery			
Phenanthrene d-10	52	52	52

Table 4: Radiocarbon dating results. Radiocarbon ages are presented in ^{14}C values while intercept, 1 sigma, and 2 sigma values are represented in calendar years before present (Cal. year BP).

Sample (Depth in cm)	Radiocarbon Age (Year BP)	Intercept (Cal. Year BP)	1 sigma	2-Sigma
80	795 +/- 100 BP	740	869-899	631-925
106	1720 +/- 20 BP	1,624	1595-1628	1563-1638
123	440 +/- 20 BP	506	499-513	484-522
210	4220 +/- 20 BP	4,823	4820-4840	4811-4846
224	10700 +/- 170 BP	12,600	12413-12762	12110-12971

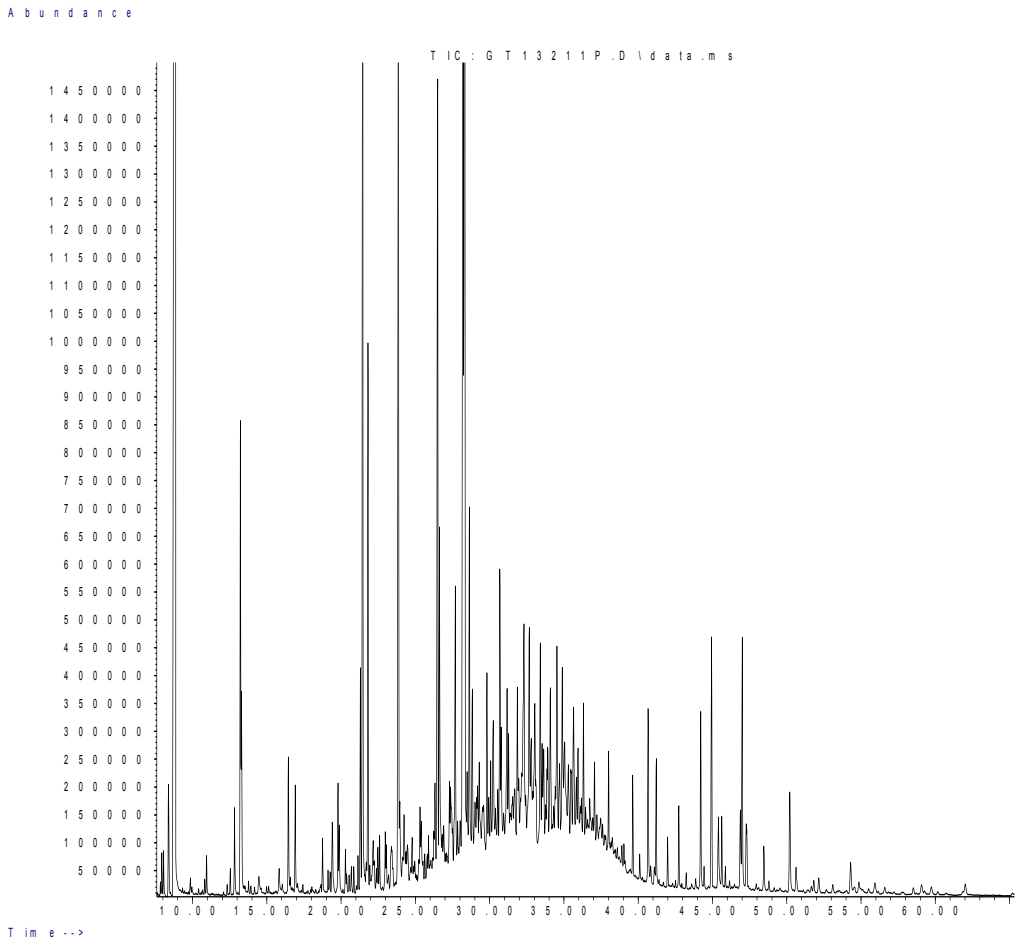

Figure 18: Total ion chromatogram for dry extraction sample A1.

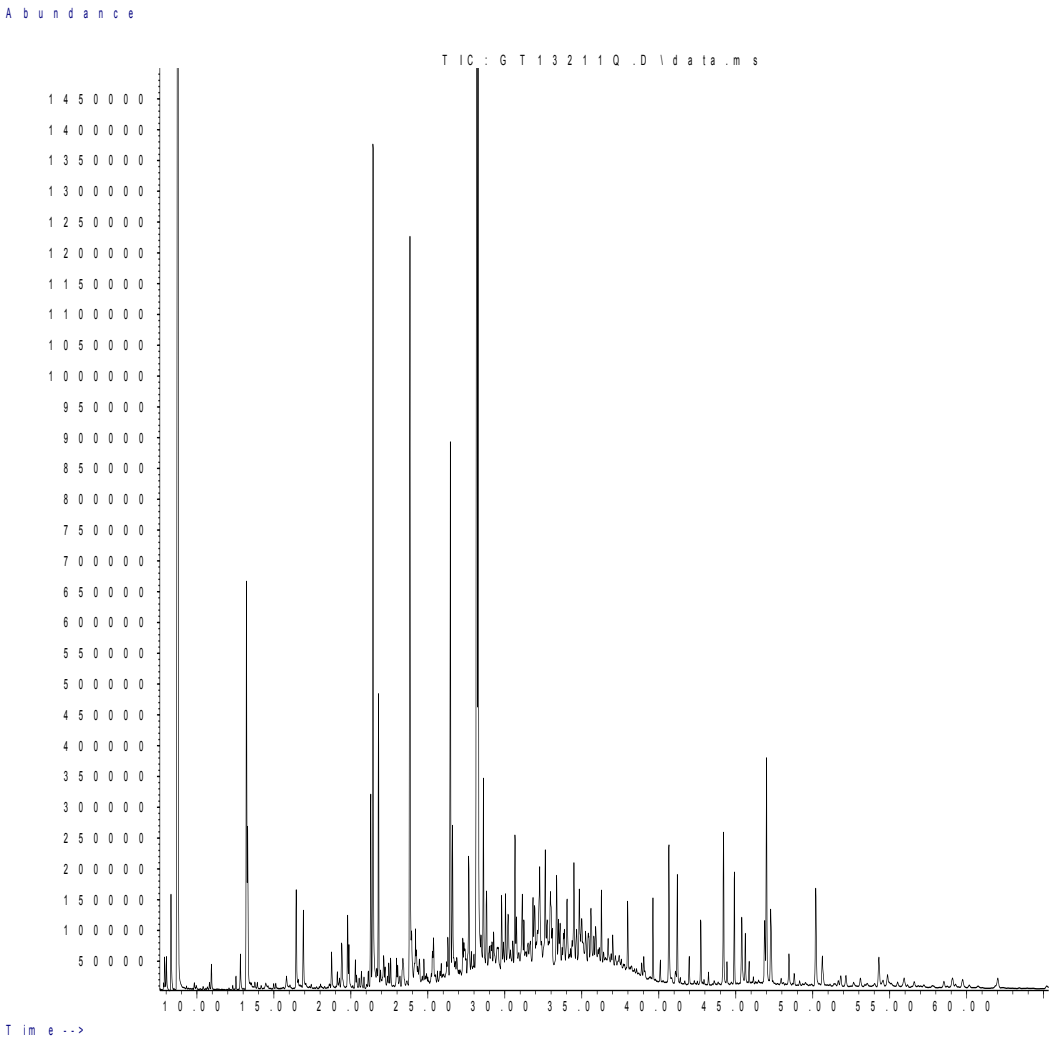

Figure 19: Total ion chromatogram for dry extraction sample A2.

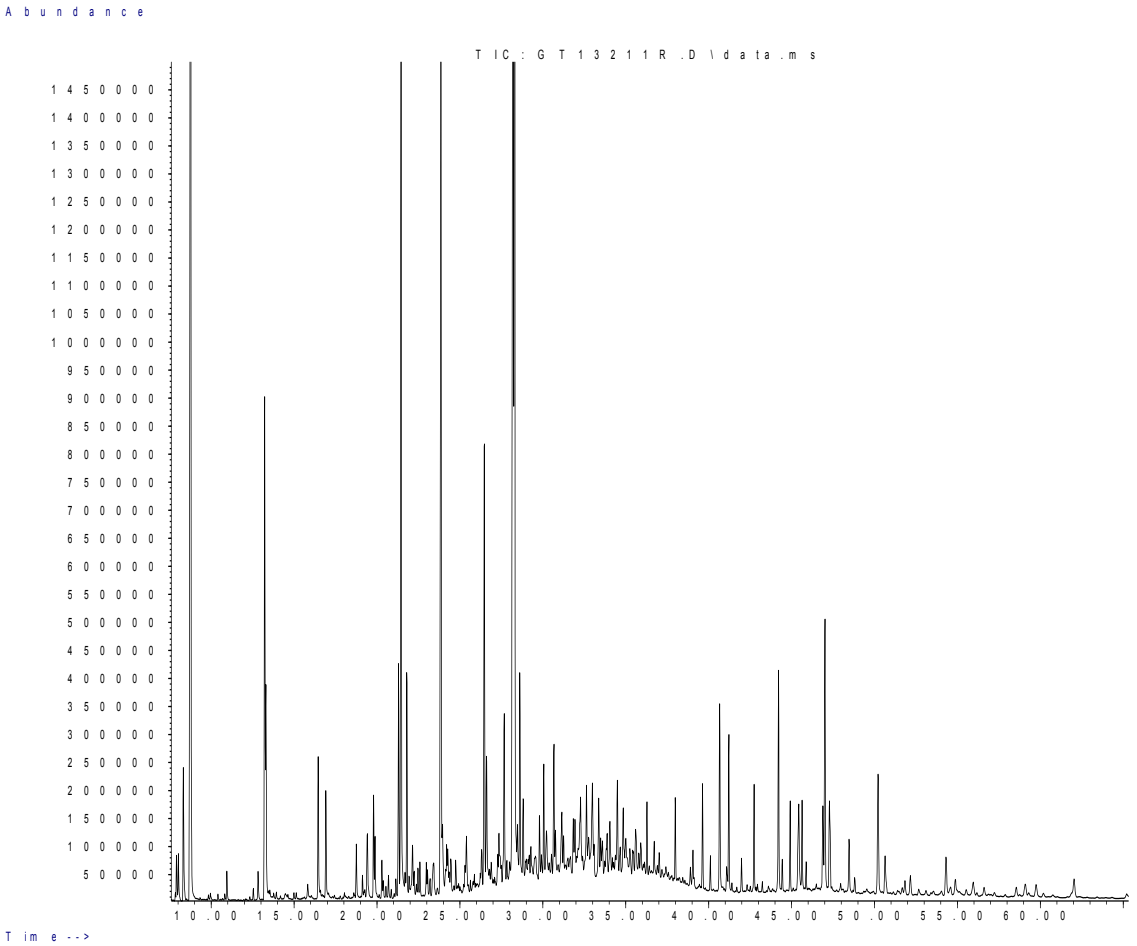

Figure 20: Total ion chromatogram for dry extraction sample A3.

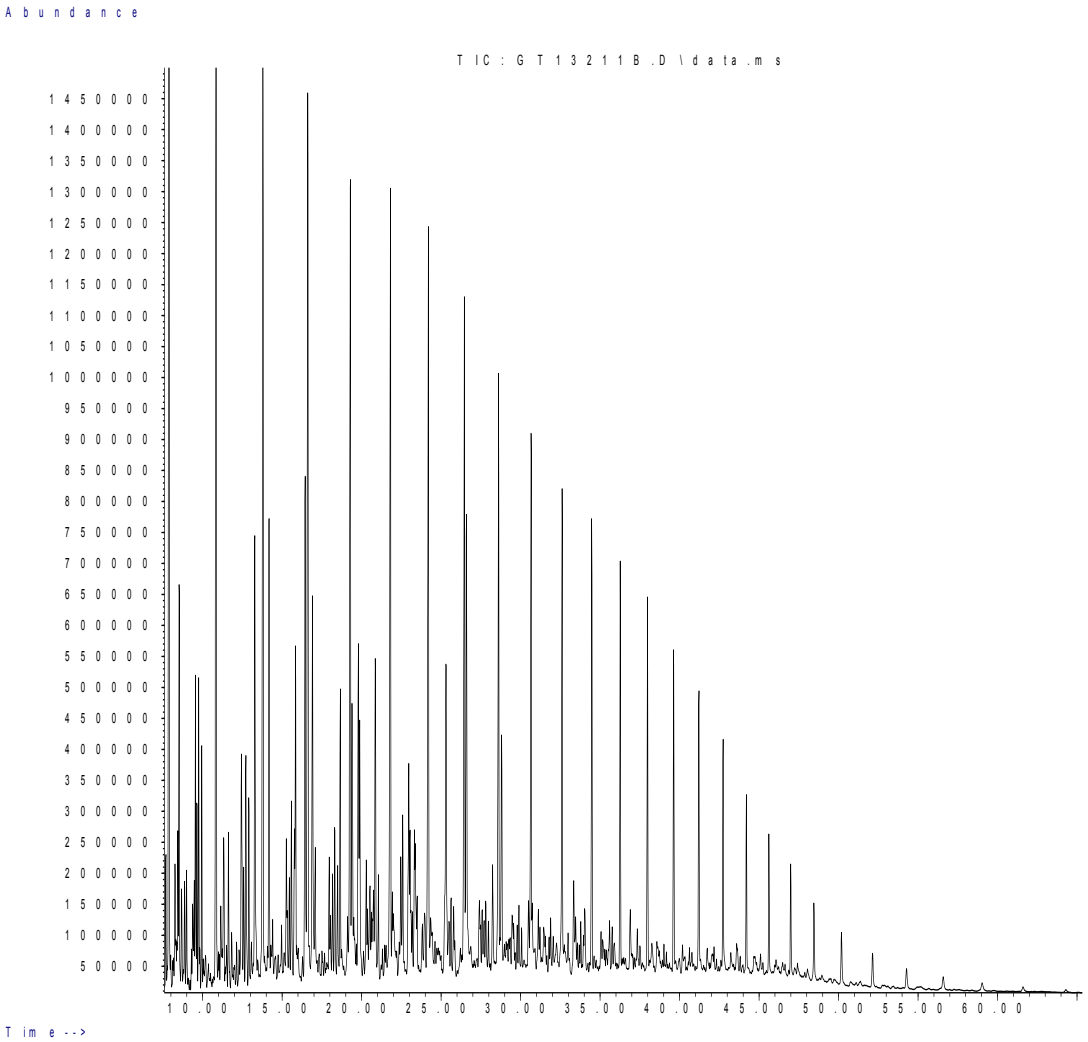

Figure 21: Source MC252 total ion chromatogram.

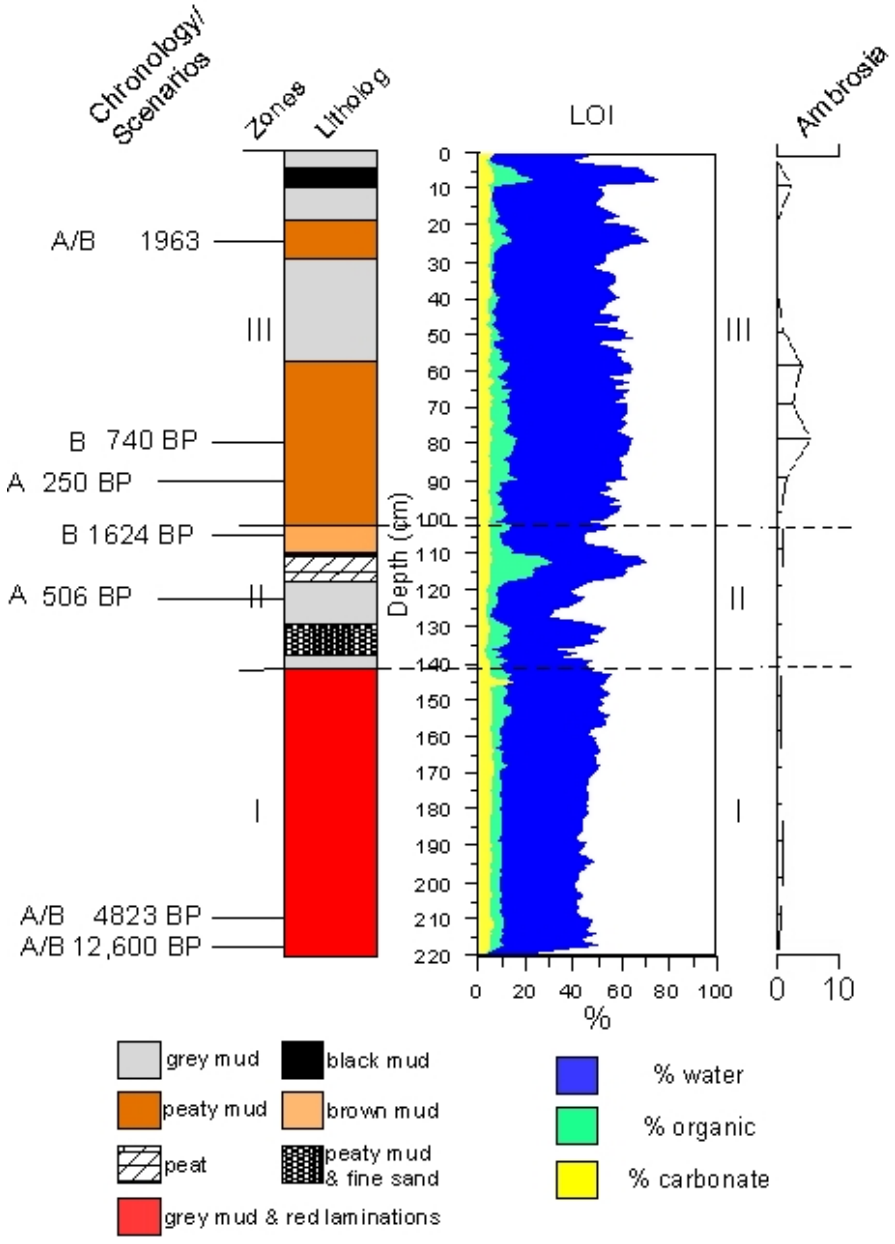

Figure 22: LOI and *Ambrosia* curve used to establish a reliable chronology of BC53. Scenario A incorporates radiocarbon dating, Ambrosia rise, and ^{137}Cs peak. Scenario B displays two radiocarbon dates out of sequence (740 and 1624 BP).

CHAPTER 6. DISCUSSION

6.1 Establishing a Reliable Chronology

According to the Oxford Handbook of Wetland Archaeology, establishing a reliable chronology in a wetland through radiocarbon dating analysis can be problematic. The chronology establishment in Core BC53 was challenging, as two samples (80 cm and 106 cm, Figure 18) are out of sequence within the stratigraphy. Therefore, two scenarios (A and B) are presented (Figures 20, 21). Since ^{137}Cs dating is a robust technique and the profile shows a distinct curve, it is used in both scenarios. Scenario B is based on the assumption that materials extracted at 80 and 106 cm were contaminated by older reworked materials carried by floodwaters over the bank of Bayou Lafourche and deposited at the coring site, thus displaying an inaccurate representation for dating. Although the two bottom most radiocarbon samples (210 and 218 cm) seem unreasonable, it is possible that the sample at 218 cm (12,600 year BP) was derived from a Pleistocene surface. During that time, the Caminada-Moreau headland existed as a Chenier complex characterized by a series of aeolian-derived sand dunes (Saucier, 1994). The sample from 210 cm (4823 year BP) represents the time at which the site transitioned from a dune to a lagoon. Scenario A contains an approximate date of 250 BP, represented by the prominent spike in *Ambrosia* at 96 cm. The correlation between deforestation, increased agricultural practices, and an increase in invasive weedy taxa such as *Ambrosia* has been regionally documented (McAndrews, 1988; Reese and Liu, 2001). The increase in *Ambrosia* within the study site can be interpreted to mark the

settlement of Grand Isle, Louisiana in the mid-1700s (Cowan et al., 1983). This evidence supports scenario A as a more likely chronological scenario for the core.

6.2 Zone I: Lafourche Delta/Floodplain Stage

Due to the absence of inorganic sediment in Zone I, this was during the active period of the Lafourche delta. This was a phase of typical fluvial deposition, occurring before the abandonment of the Lafourche delta. This is supported by constant LOI data and high percentages of *Pinus*. *Pinus* is representative as a regional pollen component transported to the coring site via the Mississippi River (Chmura and Liu, 1990). The presence of interspersed reddish brown laminations throughout this zone suggests that this was a period in which the coring site probably existed as a floodplain or backswamp environment influenced by the Red River (Aslan, Autin, and Blum 2005). During this time, the Red River was conjoined to the Mississippi River and contributed to the sediment deposition of the Lafourche delta. The decrease in Amaranthaceae is not indicative of a drop in sea level, but is likely due to the increases in *Typha* and *Poaceae* at the depths within Zone I. The high concentrations of Poaceae and *Typha* further indicate a freshwater environment. Local sea level records indicate that sea level was likely 15 m lower than the present at 12,000 to 9,000 year BP (Suter, Berryhill, and Penland, 1987; Clark et al., 2009). The presence of dinoflagellates suggests marine intrusion at the bottom of Zone I. While the exact mechanism of deposition cannot be determined, an incoming hurricane is a likely cause. It is believed that storm surge into Bayou Lafourche could create a saltwater pulse to the study site (Li, 1994). There is no evidence of hurricane influence found within Zone I, likely due to the coring site's

distance from the ocean and the consistent sediment stock of fine grained sediments transported to the coring site at that time. Even during intense hurricane-induced flooding events, these signatures were irretrievable due to the consistent source of riverine sediment during this period.

6.3 Zone II: Hurricane-Induced Deposition/Freshwater Lagoon Stage

The lithology of Zone II indicates a much more dynamic period for Bay Champagne. The absence of red mud laminations within this zone marks the termination of the Red River-Mississippi River complex. This sequence of storms is presented in the stratigraphy in Figure 22. The well-defined decreases in LOI content (water, organics), large spikes in the Cl/Br ratio, and decreases in "terrestrial indicators" (Br, K, Co, and Zn) support the presence of hurricane influence. The elements labeled "terrestrial indicators" are associated with fine grained sediments derived from fluvial sources (Bianchette, 2014; Sabatier, 2012). Hurricane layers (A and B, Figure 22) were likely scoured from the floor of Bay Champagne and transported to the sampling site via storm surge, as these layers differ from sediments found along the seaward boundary of the lagoon (Williams, 2009). The high-organic layer positioned above the hurricane sand layer at 142-137 cm (Layer A) was not due to vegetation growth, but is likely a wrack deposit that was washed into the coring site following intense flooding. This further supports the idea proposed by Liu et al. (2011) and McCloskey and Liu (2012, 2013) concerning hurricane-induced flux of fluvial sediments to backbarrier coastal water bodies following the passage of a storm. The second hurricane deposit, Layer B (128-120 cm) is also supported by decreases in LOI

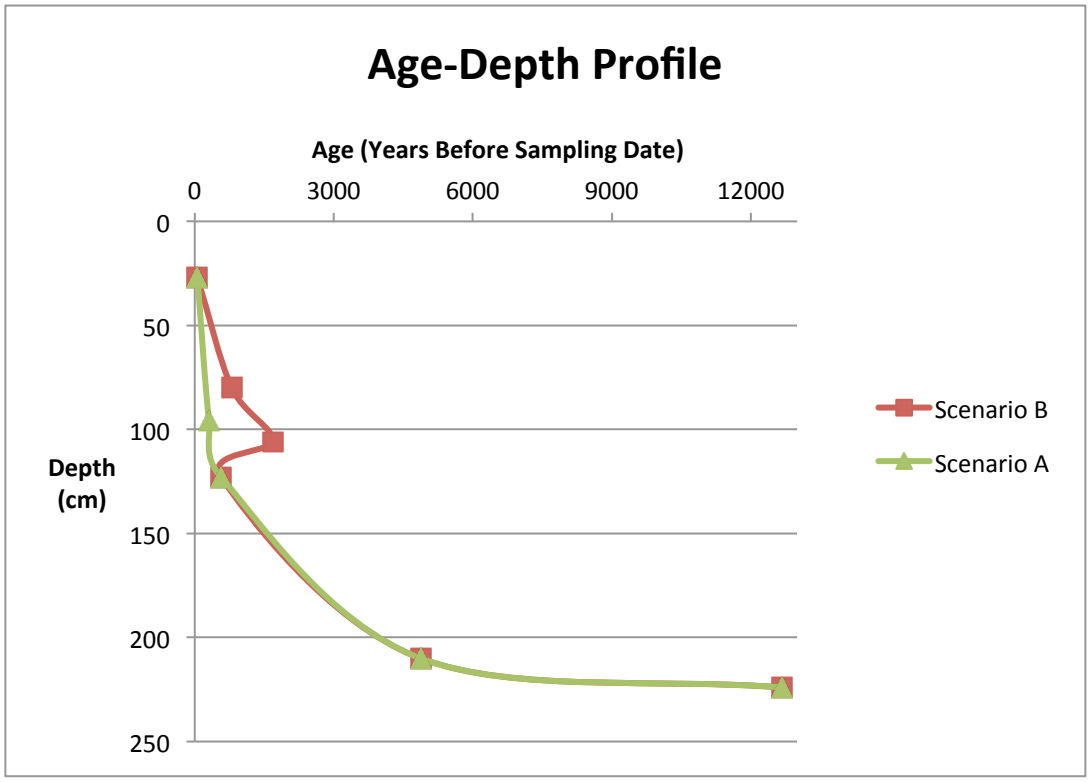

Figure 23: Age-depth profile of BC53 based on calibrated radiocarbon data and ^{137}Cs peak. Profile displays apparent sedimentation rates based on Scenarios A and B.

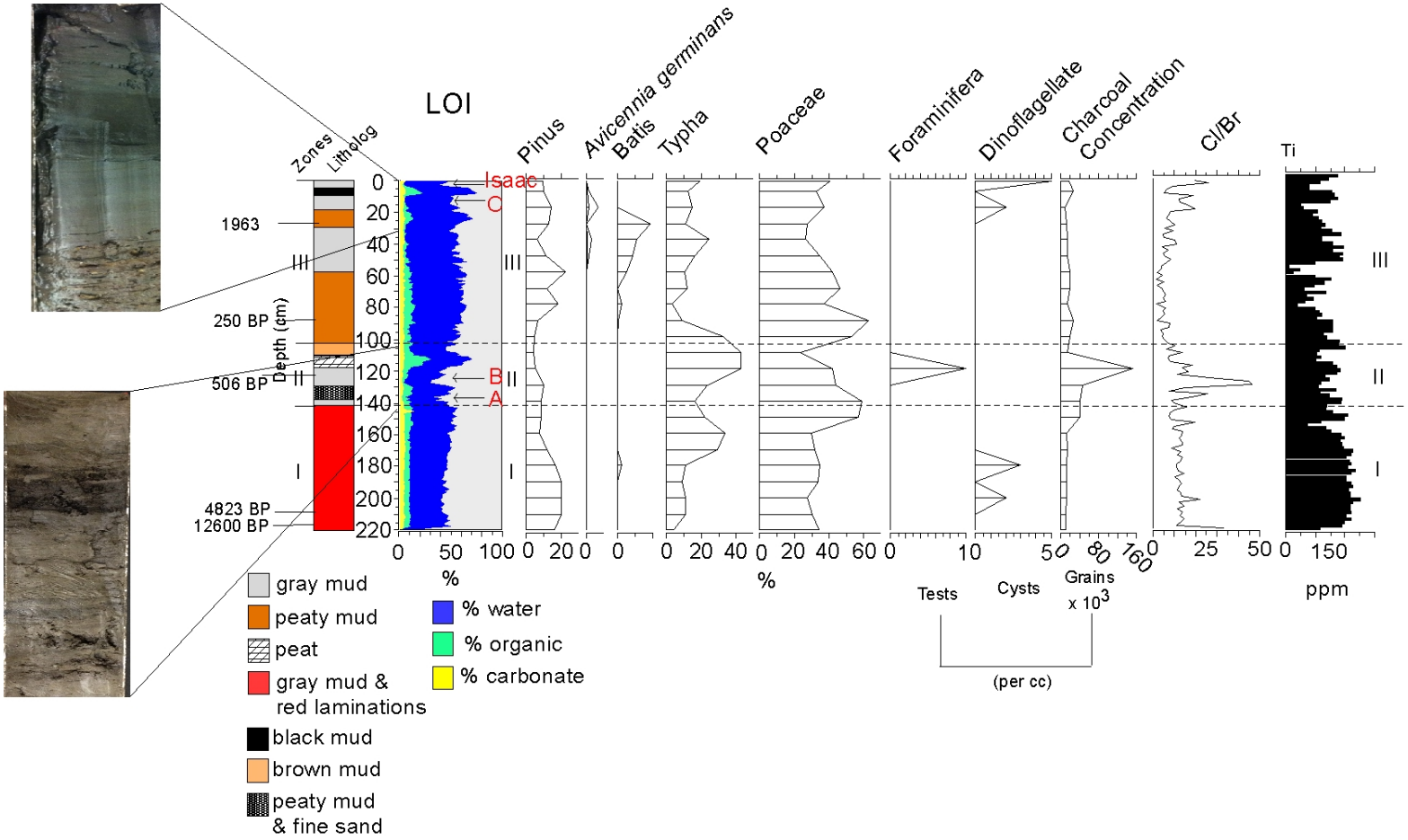

Figure 24: Data displaying paleoenvironmental change of Bay Champagne.

values, decreases in terrestrial elements, prominent increases in marine elements, and the presence of a foraminifera test. High concentrations of Poaceae coupled with low values of Amaranthaceae suggest that the site was still surrounded by freshwater marshes at this time. The 3-fold increase in charcoal concentration within the peat layer which followed the hurricane deposit at 128-120 cm is likely indicative of local fires occurring after the passage of a hurricane, as suggested by the hypothesis of hurricane-fire interactions (Liu, Lu, and Shen, 2008). The decrease in *Pinus* and increase in Poaceae and *Typha* at 106-96 cm represents the ecological succession of grass taxa following the decline of trees due to fire stress. This has been found in multiple landscape recovery studies (He and Mladenoff, 1999; He, Mladenoff, and Gustafson, 2002). The spike in Amaranthaceae at the boundary of Zones II and III indicates the transition to a more saline environment

6.4 Zone III: Transgression/Brackish Lagoon Stage

Within the past 400 years, the hydrological conditions of the lower Lafourche delta have changed drastically. Sediment compaction, reduction of fluvial sediment input, and subsidence have led to increased saltwater intrusion (Day et al., 2007, Henry and Twilley, 2013). Core BC53 has recorded these changes. The secular increase in Cl content throughout Zone III coupled with the slight overall decrease in terrestrial indicators suggests the transgression of Bay Champagne. This is reflected by the pollen evidence, as it illustrates the shift from freshwater marsh to a brackish-salt marsh environment. The increases of Amaranthaceae and *Batis*, and low values of *Typha*

within this zone, indicate vegetation shifts induced by sea level rise. The emergence of *Aviciennia germinans* at 46 cm is representative of a rise in sea level and warmer climate as their survival and replacement of salt marsh plants is directly correlated to saline environments and decreased freeze frequency (Chen and Twilley, 1998). The emergence of *Avicennia germinans* serves as not only an indicator of a rise in winter temperature and relative sea-level, but also a significant ecological change in a rapidly subsiding coast. The replacement of herb-dominated marsh landscape by shrubby black mangroves may serve advantageously in combating coastal erosion as black mangroves possess denser root structures and higher organic production (Chen and Twilley, 1998; Henry and Twilley, 2013). Although percentages of *Avicennia* are low in comparison to other taxa, this is not representative of population density due to its low pollen production. Zone III displays two hurricane layers (C and Isaac, Figure 18). Each is denoted by decreases in water and organic percentages, increases in terrestrial indicators, and the presence of dinoflagellates. The dinoflagellates indicate marine incursion while the increases in terrestrial elements represent the fluvial flooding associated with hurricane precipitation. In respect to the stratigraphic position of the hurricane layers and the ^{137}Cs peak (27 cm), these storms occurred after 1963. Due to the dating constraint we cannot definitively link this layer to a historic storm; however, we can infer that the uppermost layer was attributed to Hurricane Isaac since the sampling date was two weeks following its landfall near the study site.

6.5 Overview

Core BC53 is lithological dominated by dark mud as noted by visual inspection and LOI. LOI, XRF, and pollen analyses revealed the sedimentary history of the Lafourche deltaic lobe during its construction and deterioration phases. Zone I captured the constructive phase as noted by high baseline concentrations of terrestrial elements, constant LOI data, and sediment signatures from the Red River, indicating fluvial deposition. Zone II is defined as the boundary at which the Red River separated from the Mississippi River. This is noted in Core BC53 and also the literature (Aslan, Autin, and Blum, 2009). Zone III represents the transgressive period of Bay Champagne and the Caminada-Moreau headland. Multiple distinct dips in terrestrial elements are present in Zone III and become more frequent as the zone progresses upward, further indicating repetitive marine influence. The upper 80 cm of Zone III show a distinct rise in Amaranthaceae including the emergence and increase of *Batis* and *Avicennia germinans*. This also suggests a rise in sea-level or increase in marine incursion.

Although Bay Champagne is known to be highly susceptible to overwash events induced by hurricanes (Liu et al., 2011; Naquin et al., 2014), Core BC53 shows limited signs of these geologic signatures due to the far distance of coring site to the beach barrier (300 m). This suggests that sand transport via hurricane overwash is constrained to the southernmost portion of the lagoon nearest the sand barrier. BC53 captured the presence of four hurricane strikes; however, the hurricane layers did not consist of material from the beach barrier, but were likely derived from suspended sediments that were reworked by storm surge from the lagoon floor. Other hurricane signatures were

deposited by flooding caused by intense precipitation that induced sediment transport from Bayou Lafourche to the coring site. LOI, XRF, and palynological data support that they were mainly sediment deposited by hurricanes.

CHAPTER 7. CONCLUSION

Pollen, LOI analysis, XRF analysis, ^{137}Cs dating, and radiocarbon dating were used to reconstruct the paleoenvironment of a rapidly retreating coastal zone of the Lafourche deltaic lobe in southern Louisiana. From 4823 to approximately 1000 year BP, the coring site represented a backswamp or freshwater marsh environment as shown by high organics, low Cl content, and high percentages of *Typha* and Poaceae. At about ca. 600-400 year BP, the sampling site still existed as a freshwater marsh as indicated by an assemblage high in Poaceae and low in Amaranthaceae. During this prehistoric period, two hurricanes affected the area, which were identified by decreases in LOI content, spikes in the Cl/Br ratio, and the presence of a foraminifera test. The first hurricane likely generated an intense storm surge inundating the region, forming a thin storm deposit in the stratigraphy. This was followed by a wrack layer moved by Bayou Lafourche and nearby flooded marshes (Cahoon et al., 1995). The second hurricane was probably more severe, as suggested by a thicker storm deposit marked by the presence of foraminifera as well as a prominent spike in marine chemical elements (especially Sr) and in the Cl/Br ratio. Bay Champagne has been shown to be sensitive to freshwater influxes following the passage of a hurricane in the recent past (Liu et al., 2011). The high concentration of charcoal found within this layer followed by a decrease in arboreal pollen represents fire disturbance fueled by the decay of trees damaged by hurricanes (Liu, Lu, and Shen, 2008). Approximately, the 400 years of stratigraphy shows that the site has been subjected to significant sea-level rise. This is reflected by the overall increase of Cl and decrease in water content. The emergence of *Batis* and *Avicennia*

germinans, and the shift to salt marsh (Amaranthaceae) approximately 120 years ago, can be correlated to relative sea-level rise due to the subsidence of the Lafourche delta and global sea level rise. Another series of hurricane layers were found within the upper depths of the core. Due to their stratigraphic position in relation to the ^{137}Cs peak, these storms affected the area within the past 50 years. Hurricane Isaac probably deposited the uppermost clastic layer found in Core BC53. This layer can serve as a modern analog in future paleotempestological studies.

While this study is the first to document long-term paleoenvironmental changes in the Lafourche delta, more research is warranted for this region. Evaluating a series of sediment cores taken from the mangrove-covered marsh north of Bay Champagne may provide additional datasets to corroborate results from this study. It is widely accepted that the Caminada-Moreau headland is subjected to rapid rates of subsidence and further paleoenvironmental records could be used to inform policymakers to broaden the scope on coastal management of Port Fourchon region. Understanding the ecological shifts in local and regional vegetation such as the emergence and migration of *Avicennia germinans* is vital for sound decision-making for coastal zone management in this region.

BIBLIOGRAPHY

Aslan, A., Autin, W.J., and Blum, M.D. (2005). Causes of river avulsion: Insights from the late Holocene avulsion history of the Mississippi River, USA. Journal of Sedimentary Research. 75; 650-664.

Atkinson, T.C., Briffa, K.R., and Coope, G.R. (1987). Seasonal temperatures in Britain during the past 22,000 years, reconstructed using beetle remains. Nature. 325; 587-592.

Bai, X., Zhang, X., and Wang, S. (2011). The application of caesium-137 measurements to estimate recent sedimentation rates in a typical karst depression of Guizhou Plateau, China. Chinease Journal of Geochemistry. 30-84-92 Beget, J.E. (1983). Radiocarbon-dated evidence of worldwide early Holocene climate change. Geology. 11; 389-393.

Bianchette, T.A. (2014). Holocene paleoenvironmental reconstruction from Mexico's Pacific coast: A paleotempestological investigation. PhD dissertation. Louisiana State University, Baton Rouge, LA.

Blum, M.D., Guccione, M.J., Wysocki, D.A., Robnett, P.C., and Rutledge, E.M. (2000). Late Pleistocene evolution of the lower Mississippi River valley, southern Missouri to Arkansas. Geological Society of America Bulletin. 112; 221-235.

Blum, M.D. and Roberts, H.H. (2009). Drowning of the Mississippi Delta due to insufficient sediment supply and global sea-level rise. Nature Geoscience. 10; 488-491.

Bond, G., Showers, W., Cheseby, M., Lotti, R., Almasi, P., deMenocal, P., Priore, P., Cullen, H., Hajdas, I., and Bonani, G. (1997). A pervasive millennial-scale cycle in North Atlantic Holocene and glacial climates. Nature. 278; 1257-1266.

Bond, G., Kromer, B., Beer, J., Muscheler, R., Evans, M.N., Showers, W., Hoffmann, S., Lotti-Bond, R., Hajdas, I., and Bonani, G. (2001). Persistent solar influence on North Atlantic climate during the Holocene. Science. 294; 2130-2136

Broecker, W.S. (2006). Was the Younger Dryas Triggered by a Flood? Science. 312; 1146-1148.

Brown, P.A., and Kennett, J.P. (1998). Megaflood erosion and meltwater plumbing changes during last North American deglaciation recorded in Gulf of Mexico sediments. Geology. 26; 599-602.

Brown, K.M. and Swearingen, D.C. (1998). Effects of seasonality, length of immersion, locality, and predation on an intertidal fouling assemblage in the Northern Gulf of Mexico. Ecology. 225; 107-121.

Cahoon, D.R., Hensel, P.F., Spencer, T., and Reed, D.J. (2006). Coastal wetland vulnerability to relative sea-level rise: wetland elevation trends and process controls. In: Wetlands and Resource Management. New York: Springer-Verlag Berlin Heidelberg.

Cahoon, D.R., Reed, D.J., Day, J.W., Steyer, G.D., Boumans, R.M., Lynch, J.C., McNally, D., and Latif, N. (1996). The influence of Hurricane Andrew on sediment distribution in Louisiana coastal marshes. Journal of Coastal Research. Special Issue 21; 280-294.

Chen, R., and Twilley, R.R. (1998). A gap dynamic model of mangrove forest development along gradients of soil salinity and nutrient resources. Journal of Ecology. 86; 37-52.

Chmura, G.L. and Liu, K-b. (1990). Pollen in the lower Mississippi River. Review of Paleobotany and Palynology. 64; 253-261.

Clark, P.U., Dyke, A.S., Shakun, J.D., Carlson, A.E., Clark, J., Wohlfarth, B., Mitrovica, J.X., Hostetler, S.W., and McCabe, A.W. (2009). The Last Glacial Maximum. Science. 235; 710-714.

Coleman, J.M. (1988). Dynamic changes and processes in the Mississippi River delta. Geological Society of America Bulletin, 100; 999-1015.

Cowan, W.G., Chase, J.C., Dufour, C.L., LeBlanc, O.K., and Wilds, J. (1983). New Orleans yesterday and today: A guide to the city. Baton Rouge, LA: Louisiana State University Press.

Cupples, W., and Van Arsdale, R. (2014). The preglacial “Pliocene” Mississippi River. Journal of Geology. 122; 1-15.

Day et al. (2000). Pattern and process of land loss in the Mississippi Delta: A spatial and temporal analysis of wetland habitat change. Estuaries, 23; 425-438.

Day et al. (2007). Restoration of the Mississippi Delta: Lessons from Hurricanes Katrina and Rita. Science, 315; 1679-1684.

Deevey, E.S. and Flint, R.F. (1957). Postglacial hypsithermal interval. Science. 125; 182-184

Domack, E.W., Jull, T., and Nakao, S. (1991). Advance of East Antarctic outlet glaciers during the Hypsithermal: Implications for the volume state of the Antarctic ice sheet under global warming. Geology. 19; 1059-1062.

Emanuel, K. (2005). Divine Wind: The History and Science of Hurricanes. New York: Oxford Univ. Press.

Faegri, K. and Iversen, J. (1989). Textbook of Pollen Analysis. Amsterdam, Balkena.

Fairbanks, R.G. (1989). A 17,000-year glacio-eustatic sea level record: influence of glacial melting rates on the Younger Dryas event and deep-ocean circulation. Nature. 342; 637-642.

Fisk, H.N. (1956). Nearsurface sediments of the continental shelf off Louisiana. (Proceedings of the 8th Annual Conference on Soil Mechanics and Foundation Engineering). 1-36.

Fleming, K., Johnston, P., Zwartz, D., Yokoyama, Y., Lambeck, K., and Chappell, J. (1998) Refining the eustatic sea-level curve since the Last Glacial Maximum using far- and intermediate- field sites. Earth and Planetary Science Letters. 163; 327-342.

Gosselink, J.G. (1984). The ecology of delta marshes of coastal Louisiana: A community profile. U.S. Fish Wildlife Service. FWS/OBS-84/09. 134 pp.

Grove, J.M. and Switzur, R. (1994). Glacial evidence for the Medieval Warm Period. Climatic Change. 26; 143-169.

He, S.H. and Mladendoff, D.J. (1999). Spatially explicit and stochastic simulation of forest-landscape fire disturbance and succession. Ecology. 80; 81-99.

He, S.H., Mladendoff, D.J., and Gustafson, E.J. (2002). Study of landscape change under forest harvesting and climate warming-induced fire disturbance. Forest Ecology and Management. 155; 275-270.

Henry, K.M., and Twilley, R.R. (2013). Soil development in a coastal Louisiana wetland during a climate-induced vegetation shift from salt marsh to mangrove. Journal of Coastal Research. 29; 1273-1283.

Hoek, W.Z. (1997). Paleogeography of Lateglacial Vegetations. Amsterdam.

Johnsen, S.J., Clausen, H.B., Dansgaard, W., Fuhrer, K., Gundestrup, N., Hammer, C.U., Iversen, P., Jouzel, J., Stauffer, B., and Steffensen, J.P. (1992). Irregular glacial interstadials recorded in a new Greenland ice core. Nature. 359; 311-313.

Kehew, A.E. and Lord, M.L. (1987). Sedimentology and paleohydrology of glacial-lake outburst deposits in southeastern Saskatchewan and northwestern North Dakota. Geological Society of America Bulletin. 99; 663-673.

Kesel, R.H., Dunne, K.C., McDonald, R.C., Allison, K.R., and Spicer, B.E. (1974). Lateral erosion and overbank deposition on the Mississippi River in Louisiana caused by 1973 flooding. Geology. 2; 461-464.

Kutzbach, J.E. (1985). Milankovich forcing of fluctuations in the level of tropical lakes from 18 to 0 kyr BP. Nature. 317; 130-134.

Lambeck, K., Yokoyama, Y., and Purcell, T. (2002). Into and out of the Last Glacial Maximum: sea-level change during Oxygen Isotope Stages 3 and 2. Quaternary Science Reviews. 21; 343-360.

Li, X. (1994). A 6200-year environmental history of the Pearl River marsh, Louisiana. PhD Dissertation. Louisiana State University, Baton Rouge, LA.

Liu, K.-b. and Fearn, M.L. (1993). Lake-sediment record of late Holocene hurricane activities from coastal Alabama. Geology, 21: 793-796.

Liu, K.-b. and Fearn, M.L. (2000). Holocene history of catastrophic hurricane landfalls along the Gulf of Mexico coast reconstructed from coastal lake and marsh sediments. In: Ning, Z. and Abdollahi, K. (Eds.): Current Stresses and Potential Vulnerabilities: Implications of Global Change for the Gulf Coast Region of the United States. Baton Rouge, Franklin, 38-47.

Liu, K.-b. (2004). Principles, methods, and examples from Gulf coast lake sediments. In: Murnane, R. and Liu, K.B. (Eds.): Hurricanes and Typhoons: Past, Present, and Future. New York, Columbia University Press, 13-57.

Liu, K.-b. (2013). Paleotempestology. In: Elias, S. (Ed.): Encyclopedia of Quaternary Science. Amsterdam, Elsevier, 209-221.

Liu, K-b, Li, C., Bianchette, T.A., McCloskey, T.A., Yao, Q., and Weeks, E. (2011). Storm deposition in a coastal backbarrier lake in Louisiana caused by Hurricanes Gustav and Ike. Journal of Coastal Research, SI 64 (Proceedings of the 11th International Coastal Symposium), 1866-1870.

Mahowald, N., Kohfeld, K., Hansson, M., Balkanski, Y., Harrison, S.P., Prentice, I.C., Schulz, M., and Rodhe, H. (1999). Dust sources and deposition during the last glacial maximum and current climate: A comparison of model results with paleodata from ice cores and marine sediments. Journal of Geophysical Research. 104; 15895-15916.

Mann, M.E. (2002). Little Ice Age. In: MacCracken, M.C., and Perry, J.S. (Eds). The Earth System: physical and chemical dimensions of global environmental change. John Wiley and Sons, Ltd, Chincester, 2002.

McAndrews, J.H. (1988). Human disturbance of North America forests and grasslands: The fossil pollen record," in Huntley and Webb III, eds., Vegetation History. Dordrecht: Kluwer Academic Publishers.

McAndrews, J.H., Berti, A.A., and Norris, G. (1973). Key to the Quaternary pollen of the Great Lakes region. Royal Ontario Museum Miscellaneous Publications, Toronto.

McCloskey, T.A. and Liu, K-b. (2012). A sedimentary-based history of hurricane strike on the southern Caribbean coast of Nicaragua. Quaternary Research. 78; 454-464.

McCloskey, T.A. and Liu, K-b. (2013). A 7000 year record of paleohurricane activity from a coastal wetland in Belize. The Holocene. 23; 278-291.

Menotti, F. and O' Sullivan, A. (2012). The Oxford Handbook of Wetland Archaeology. Oxford University Press.

Michot, T.C., Day, R.H., and Wells, C.J. (2010). Increase in black mangrove abundance in coastal Louisiana. Louisiana Natural Resources News (Newsletter of the Louisiana Association of Professional Biologists). 2010; 4-5

Murton, J.B., Bateman, M.D., Dallimore, S.R., Teller, J.T., and Yang, Z. (2010). Identification of Younger Dryas outburst flood path from Lake Agassiz to the Arctic Ocean. Nature. 464; 740-743.

Neill, C. and Deegan, L.A. (1986). The effect of Mississippi River delta lobe development on the Habitat composition and diversity of Louisiana Coastal Wetlands. American Midland Naturalist. 116; 296-303.

Naquin, J.D., Liu, K-b., McCloskey, T.A., and Bianchette, T.A. (2014). Storm Deposition Induced by Hurricanes in a Subsiding Coastal Zone. In: Green, A.N. and Cooper, J.A.G. (eds.), Proceedings 13th International Coastal Symposium(Durban, South Africa), Journal of Coastal Research, Special Issue No. 70; 308-313.

Penland, S. and Ritchie, W. (1979). Short-term morphological changes along the Caminada-Moreau coast, Louisiana: Trans. Gulf Coast Association. Geological Societies. 29; 342-346.

Penland, S., Boyd, R., and Suter, J. (1988). Transgressive depositional systems of the Mississippi Delta Plain: A model for barrier shoreline and shelf sand development. Journal of Sedimentary Petrology, 58: 932-949.

Penland, S. and Ramsey, K.E. (1990). Relative sea-level rise in Louisiana and the Gulf of Mexico: 1908-1988. Journal of Coastal Research. 6; 323-342.

Penland, S., Connor, P.F., Beall, A., Fearnley, S., and Williams, S.J. (2005). Changes in Louisiana's shoreline: 1855-2002. Journal of Coastal Research. 25; 253-269.

Poore, R.Z., DeLong, K.L., Richie, J.N., and Quinn, T.M. (2009). Evidence of multidecadal climate variability and the Atlantic Multidecadal Osciallation from a Gulf of Mexico sea-surface temperature-proxy record. Geo-Marine Letters. 29; 477-484.

Reese, C.A. and Liu, K-b. (2001). Late-Holocene vegetation changes at Bluff Swamp, Louisiana. Southern Geographer. 41; 20-35.

Richie, J.N., Poore, R.Z., Flower, B.P., and Quinn, T.M. (2007). 1400 yr multiproxy record of climate variability from the northern Gulf of Mexico. Geology. 35; 423-426.

Rittenour, T.M., Blum, M.D., and Goble, J.R. (2007). Fluvial evolution of the lower Mississippi River valley during the last 100 k.y. glacial cycle: Response to glaciation and sea-level change. Geological Society of America Bulletin. 119; 586-608.

Roberts, H.H. (1997). Dynamic changes of the Holocene Mississippi River delta plain: The Delta Cycle. Journal of Coastal Research. 13; 605-627.

Saucier, R.T. (1994). Geomorphology and quaternary geologic history of the lower Mississippi valley. US Army Corps of Engineers Report. Vol 1.

Scruton, P.C. (1960). Delta building and the deltaic sequence. In: Shepard, F.P. et al. Recent sediments, northwest Gulf of Mexico. Tulsa, Oklahoma. American Association of Petroleum Geologists. 82-102.

Stuiver, M. and Braziunas, T.F. (1989). Atmospheric ^{14}C and century-scale solar oscillations. Nature. 338; 405-408.

Suter, J.R., Berryhill, H.L., and Penland, S. (1987). Late Quaternary sea-level fluctuations and depositional sequences, southwest Louisiana continental shelf. The Society of Economic Paleontologist and Mineralogists. 12; 199-219

Turner, R.E. (1991). Tide guage records, water level rise, and subsidence in the northern Gulf of Mexico. Estuaries. 14; 139-147

Urrego, L. E., G. Bernal, and J. Polania. 2009. Comparison of pollen distribution patterns in surface sediments of a Colombian Caribbean mangrove with geomorphology and vegetation. Review of Palaeobotany and Palynology 156; 358-375.

Villalba, R. (1994). Tree-ring and glacial evidence for the Medieval Warm Epoch and the Little Ice Age in Southern South America. Climatic Change. 26; 183-197.

Visser, J.M., Sasser, C.E., Charbreck, R.H., and Linscombe, R.G. (1998). Vegetation types of the Mississippi River Deltaic Plain. Estuaries. 21; 818-828.

Watchorn, M.A., Hamilton, P.B., Anderson, T.W., Roe, H.M., and Patterson, R.T. (2007). Diatoms and pollen used as indicators of water quality and land-use change: a case study from the Oak Ridges Moraine, Southern Ontario, Canada. Journal of Paleolimnology. 39; 491-509.

Williams, H.F.L. (2009). Stratigraphy, sedimentology, and microfossil content of Hurricane Rita storm surge deposits in Southwest Louisiana. Journal of Coastal Research. 25; 1041-1051.

Yokoyama, Y., Lumbeck, K., De Deckker, P., Johnston, P., and Fifield, K.L. (2000). Timing of the Last Glacial Maximum from observed sea-level minima. Nature. 406; 713-716.

VITA

James “Dustin” Naquin, native of Prairieville, LA, was born in March 1990. Following high school graduation, he moved to Baton Rouge to pursue a Bachelor of Science degree while majoring in Coastal Environmental Science with a minor in Chemistry. Beginning in the Fall 2011 semester, Dustin began working under Dr. Kam-biu Liu as a student worker in the Department of Oceanography and Coastal Sciences. After much interest in Dr. Liu’s research, he completed an independent study required for his undergraduate degree under him and was allowed to continue working in the Global Change and Coastal Paleoecology lab as a graduate student to complete a Master’s degree in Oceanography and Coastal Sciences. From December 2012 to December 2014, Dustin has worked as a graduate teaching assistant and research assistant for the Department of Oceanography and Coastal Sciences. He has presented oral presentations at an international (International Coastal Symposium; Durban, South Africa) and national conference (Geologic Society of America; Vancouver, BC, Canada) while obtaining outside sources of funding for each. Dustin has authored a published paper in the Journal of Coastal Research titled “Storm Deposition Induced by Hurricanes in a Rapidly Subsiding Coastal Zone”.